NANO · MICRO small
www.small-journal.com

Nanoarchitectonics for Abused-Drug Biosensors

Rasoul Moradi, Nazila Pour Khalili, Ni Luh Wulan Septiani, Chia-Hung Liu, Esmail Doustkhah, Yusuke Yamauchi,* and Slava V. Rotkin*

Rapid, accessible, and highly accurate biosensors for the detection of addictive and abused drugs are needed to reduce the adverse personal and societal impacts of addiction. Modern sensors that utilize next-generation technologies, e.g., nanobiotechnology and nanoarchitectonics, have triggered revolutionary progress in the field as they allow accurate detection and tracking of trace levels of major classes of drugs. This paper reviews advances in the field of biosensors for the detection of commonly abused drugs, both prescribed such as codeine and morphine, and illegal narcotics like cocaine.

1. Introduction

Abuse of prescription and illicit drugs is a major health issue worldwide. An epidemic of drug overdose deaths has been reported in the U.S.A. where fatal overdoses increased by 137% from 2000 to 2014.[1] The role of opioids in these deaths has been highlighted several times, for instance, by a White House Summit in August 2014.[1–4] At present, overdose deaths are mainly caused by opioids (including prescription opioids, heroin, and synthetic opioids such as fentanyl and its chemical analogs). Illicit drugs cause damaging lifetime alterations in the brain, making it very difficult to overcome the addiction without specialized, medical assistance. Drug addiction is a long-lasting, reverting psychiatric disorder and is a major public health issue affecting many elements in society such as health care, productivity, policing, crimes, and accidents. According to 2008 estimations, roughly, 4 million people are using opium globally and 80% of them are living in Asia. Studies have shown a link between opium use and diverse adverse health effects such as different types of cancers including oral, bladder, lung, and gastric cancers.[5–7] Opioid derivatives, morphine, codeine, fentanyl, or buprenorphine are effective analgesics for post-operative and cancer pain relief but several studies have highlighted the link between their long-term administration and high abuse potential.[8] Morphine is the most potent analgesic for chronic pain; however, its clinical use is restricted since the opiate naturally brings about tolerance and has severe withdrawal symptoms with a high risk of relapse. Over-the-counter

R. Moradi, N. P. Khalili
Nanotechnology Laboratory
School of Engineering and Applied Science
Khazar University
Baku Az1096, Azerbaijan

R. Moradi
Department of Chemical Engineering
School of Engineering and Applied Science
Khazar University
Baku Az1096, Azerbaijan

N. P. Khalili
Center for Cell Pathology Research
Department of Biological Science
Khazar University
Baku Az1096, Azerbaijan

N. L. W. Septiani
Advanced Functional Materials Research Group
Institut Teknologi Bandung
Bandung 40132, Indonesia

C.-H. Liu
Department of Urology
School of Medicine
College of Medicine, and TMU Research Center of Urology and Kidney
Taipei Medical University
No. 250, Wu-Hsing Street, Taipei 110, Taiwan

The ORCID identification number(s) for the author(s) of this article can be found under https://doi.org/10.1002/smll.202104847.

C.-H. Liu
Department of Urology
Shuang Ho Hospital
Taipei Medical University
No. 291, Zhongzheng Road, Zhonghe District, New Taipei City 23561, Taiwan

E. Doustkhah
International Center for Materials Nanoarchitechtonics (WPI-MANA)
National Institute for Materials Science
1-1 Namiki, Tsukuba, Ibaraki 305-0044, Japan
E-mail: DOUSTKHAH.esmail@nims.go.jp

E. Doustkhah, Y. Yamauchi
JST-ERATO Yamauchi Materials Space-Tectonics Project and
International Center for Materials Nanoarchitectonics (WPI-MANA)
National Institute for Materials Science (NIMS)
1-1 Namiki, Tsukuba, Ibaraki 305-0044, Japan

Y. Yamauchi
School of Chemical Engineering and Australian Institute for Bioengineering and Nanotechnology (AIBN)
The University of Queensland
Brisbane, QLD 4072, Australia
E-mail: y.yamauchi@uq.edu.au

S. V. Rotkin
Department of Engineering Science and Mechanics
Materials Research Institute
The Pennsylvania State University
Millennium Science Complex
University Park, PA 16802, USA

DOI: 10.1002/smll.202104847

(OTC) Codeine, or 3-methylmorphine, is a short-acting, weak to mid-range opioid.[9] Studies have reported that the harms associated with excessive and/or long-term use of codeine-containing medicines[10] often happen in people without any history of substance use disorders or comorbidity.[11]

The development of portable devices for easy, selective, sensitive, and cost-effective detection of abused drugs in complex biological environments facilitates early recognition, improves treatment outcomes, and can help prevent relapses.[12] Currently, drug abuse detection requires analysis of biological samples such as urine or blood in clinical laboratories or relies upon self-reporting.[13] Classical lab-based methods for monitoring abused drugs (e.g., cocaine, heroin, and morphine) range from simple chemical color tests such as thin-layer chromatography (TLC) to complex techniques like gas chromatography-mass spectrometry (GC-MS), and liquid chromatography-mass spectrometry (LC-MS). These well-established methods are reliable and accurate but are time-consuming, expensive, difficult to operate, which makes them unsuitable for on-site and real-time monitoring of abused drugs. In addition, these analytical methods may require pretreatment, clean-up, and sample preparation steps that can only be conducted in a laboratory.[14,15] To address these limitations, novel biosensors have been developed that offer promising solutions owing to their unique sensing properties.[16] A biosensor is a physical or chemical sensor that couples biological sensing materials as receptors with appropriate signal transducers.[17] Biosensors have several advantages including speed, accuracy and sensitivity and reduced costs and because they do not require advanced equipment, analyte detection can be performed at the point of care. Biosensors allow quantitative analysis of chemical species such as abused drugs in biological samples including blood, salvia, sweat, and urine.[18,19] At present, various types of biosensor technologies (e.g., electrochemical, optical, piezoelectric, magnetic, and thermometric) are being investigated for drug detection.[20–22] In addition, hybrid technologies (e.g., electrochemical/optical) have been developed recently to address the drawbacks of electrochemical biosensing of chemical compounds.[23,24] Nanotechnology-enabled biosensors sensors have been developed that allow for the selective and sensitive recognition of numerous analytes, especially stimulants and narcotics.[25] These sensors also facilitate device miniaturization through the compact integration of various micro- and nanoparts of the analytical tools, e.g., receptors, transducers, electronics, and signal processing systems, into the portable devices.[26] This approach provides novel high-throughput methods such as lab-on-chip (LOC) devices and micro-total analysis systems (μTAS), for fast and cost-effective analysis of abused drugs and relevant metabolites with very small sample volumes.[27]

A biosensor for abused drugs detection must possess the following features: high sensitivity, low cost, capability for integration in the portable platform, and multiplex analysis,[23,28] however, there are few commercialized biosensors with these features. Nevertheless, the scientific development of biosensing platforms is rapidly evolving, which is reflected in the number of recently published works.[29,30] We will review the role of biosensors in the analysis of common drugs, covering the last three decades of advances and efforts in the field of drug abuse detection. We will focus on the most frequently abused prescription drugs e.g., morphine and codeine, and the most common illegal narcotics, e.g., cocaine and heroin. For each drug, a comprehensive review of biosensing methodologies will be provided.

Nanoarchitectonics is a promising approach for developing high-performance and reliable biosensors and devices.[31–33] Platforms based on nanomaterials architectonics have been used in electronic devices such as biosensors.[34,35] The manipulation of atoms in nanoscale, building nanocar molecules and unique materials, and employing them in electronic devices, electrosensing or/and electrobiosensing are some examples of nanoarchitectonics that have been achieved in a short time since the concept emerged.[36–38] The development of biosensor devices and their capabilities can likely be revolutionized by nanoarchitectonics. In this review, we discuss biosensor designs that are inspired by nanoarchitectonics for the detection of commonly abused drugs. We focus on biosensors that employ emerging nanoarchitectonics using nanoarchitectured materials such as carbon nanomaterials, gold nanoparticles which are utilized in conjunction with antibodies, aptamers, and enzymes.

2. Biosensors

A biosensor device consists of a small sensor with a biological material fixed on it and produces a chemical, optical, or electrical signal in response to biostimulus. Biosensor technology typically combines tools from biochemistry, molecular biology, chemistry, physics, electronics, and computer science. The design of biosensors has expanded significantly in the last two decades.[39,40] Biosensors are designed to perform the selective identification of analytes based on biological components and physicochemical detectors.[41] A series of multidisciplinary breakthroughs in fields such as chemistry, physics, biological and material sciences have led to a variety of biosensing tools with a range of analytical features.[42–45] Biosensors have been developed for applications such as pre-diagnosis of diseases in medicine and health, and detection of contaminants in the environment, toxins in water and/or foods, as well as in pharmaceutics and other fields.[46–49] However, only a few prototypes have been successfully commercialized. One of these is the glucose biosensor, with the first fiber optic biosensor based on the glucose oxidase enzyme being developed in 1982, which later evolved into an electrochemical device for commercialization.[50] Advances in biosensing technology have happened through the incorporation of emerging sciences, including nanotechnology and biotechnology, and resulted in the development of different efficient biosensor architectures and configurations.[51,52] This has facilitated the implementation of biosensors as point-of-care (POC) tools for fast and real-time analysis of pathogens as well as chemical compounds in biological samples through both in vivo and in vitro approaches.[53–55]

In general, biosensors are composed of three main parts: bioreceptor, detector, and transducer.[29] A typical bioreceptor consists of a stabilized biological system that changes properties in the presence of the analyte being measured. The measuring device, which is sensitive to these changes, produces a signal proportional to the amount or type of changes, to be subsequently recognized by electronics. Various bioreceptors are used in biosensors including antibodies, cellular receptors,

deoxyribonucleic acid (DNA), ribonucleic acid (RNA), enzymes, aptamers (oligonucleotides) or peptide molecules, microorganisms or whole cells, tissues, and synthetic receptors. In these systems, physicochemical changes at the bioreceptor level are converted into a measurable signal by the transducer. The signals sent from the transducer to the processor are amplified, analyzed, and finally converted into a unit of measured concentration by the detector.[56]

An efficient biosensor needs to have high selectivity and low detection limit to a particular analyte. Biosensors are superior to other systems that may be capable of sensing nonpolar molecules formed in tissues, as they can detect trace concentrations of such compounds. Since biosensors are based on an embedded biological recognition system, no side effects are expected. Continuous and rapid control of metabolic activities is possible using these sensors.[57]

Biosensors are divided into two main groups based on how the analytes are detected: biosensors based on indirect detection of an antigen and those in which the reactant directly reacts with the analyte. In biosensors based on indirect antigen detection, the reactant is detected by cellular receptors and antibodies on the sensor. In this group, labeled compounds, such as labeled antibodies, or compounds with catalytic properties, such as enzymes, are used as the biological elements.[58]

The first biosensing probe for detecting oxygen was developed by proposing the first membrane-covered oxygen electrode in 1954 by Clark.[59] In 1962, Clark developed the first electrochemical biosensor using an enzyme electrode with membrane entrapped glucose oxidase which is sensitive to oxygen.[60] The oxygen sensor developed by Clark was later converted to measure blood sugar by coating the surface of the electrode with an enzyme that oxidizes glucose. Similarly, by covering the electrode with an enzyme capable of converting urea to ammonium carbonate, NH^{4+}, and cyanide ion a biosensor was developed to measure the amount of urea in the blood or urine.[61–63] These biosensors employed different transducing mechanisms for signal harvesting. In the first example, blood sugar was measured via the produced electric current, i.e., via amperometric measurement, and in the second example, the urea concentration was measured based on the amount of electric charge created in the electrodes, i.e., via potentiometric mechanism.

Common types of transducers use the following strategies for detection: electrochemical, optical (luminescence, absorption, surface plasmon resonance (SPR), and surface enhanced Raman spectroscopy (SERS), mechanical (sensitivity to mass change of detector after adsorption), and thermal methods.[64] To build a stable biosensor, biological components must be attached to the transducers in a special process, called stabilization. The five major methods of stabilization are adsorption, micropacking, imprinting, cross-linking, and covalent bonding. Two factors play a critical role in designing a suitable biosensor: a suitable method of stabilizing the bioreceptor on a solid surface that increases its lifespan, sensitivity, and stability, and an appropriate transducing mechanism.

Recently, nanotechnology has accelerated growth in the field of biosensors.[65,66] Novel nanomaterials such as gold nanoparticles, quantum dots (QDs), and carbon nanotubes (CNTs) have been employed in nanobiosensors. **Figure 1** illustrates the infographic timeline of the main advances in the field of biosensors of abused drugs.

2.1. Aptamer-Based Sensors

Biological recognition elements, i.e., bioreceptors such as antibodies, enzymes, and aptamers are a versatile and effective platform for developing biosensors for the detection of small molecules such as drugs. Aptamers are short sequences of single-stranded nucleic acid (DNA or RNA) or peptides with a specific 3D structure that enables them to connect with their targets with high specificity and affinity. Small size, fast and cheap production process, biocompatibility, and high stability, make them attractive for diagnostic tools such as biosensors. Aptamer molecules as recognition elements for biosensors can be specifically designed and produced via a multistep Systematic evolution of ligands by exponential enrichment (SELEX) method. Therefore, the most crucial advantage of aptamers over antibodies is that aptamers do not need animal species for production. Consequently, they do not stimulate the immune system and there are no ethical issues with working with animals. Moreover, the small size of aptamers can create higher densities when stabilizing them on a substrate so they can be employed in high throughput screening via biochips or microarrays. The main problem with aptamer biosensors (aptasensors), is the nuclease sensitivity of aptamers as their analytical performance diminishes when applied in real matrices because of the nucleases present in biological fluids.

2.1.1. Electrochemical Sensors

A large group of biosensors is based on electrochemical transducers. Electrochemical biosensors have been widely studied and commercialized recently, due to their efficiency in detecting small molecules such as glucose. They can be also used for the detection of DNA hybridization and aptamer-target binding. Electrochemical biosensors possess high sensitivity, low power consumption, low mass, and volume requirements, work with a small amount of analyte, are low cost, and can be integrated with microelectronics for mass production. The fundamentals of DNA-based electrochemical biosensing were explored by While Palacek in 1960 but the first electrochemical DNA biosensor was only developed by Millan and Mikkelsen in 1993. The major studies on electrochemical biosensors for drugs are listed in **Table 1**. Biosensor type, employed bioreceptor, transducing procedure, and obtained limits of detection (LOD) for target drug are outlined.[67–85]

2.1.2. Optical Sensors

Optical biosensing mechanisms are based on either alteration of optical properties, including the refraction index, absorption, or the appearance of an optical response as efficient fluorescence, or light scattering, as a result of the interplay between an analyte and a receptor.[86] This generates a signal proportional to the concentration of a substance. Various biologic substances, e.g., enzymes, antibodies, antigens, receptors, nucleic acids, cells, and complete tissues, can be used as bio-recognition elements.[87] Optical biosensors are among the best sensors for determining the affinity of substances or catalytic receptors' activity. They are very sensitive and versatile, thereby enabling rapid real-time detection, and can be adapted

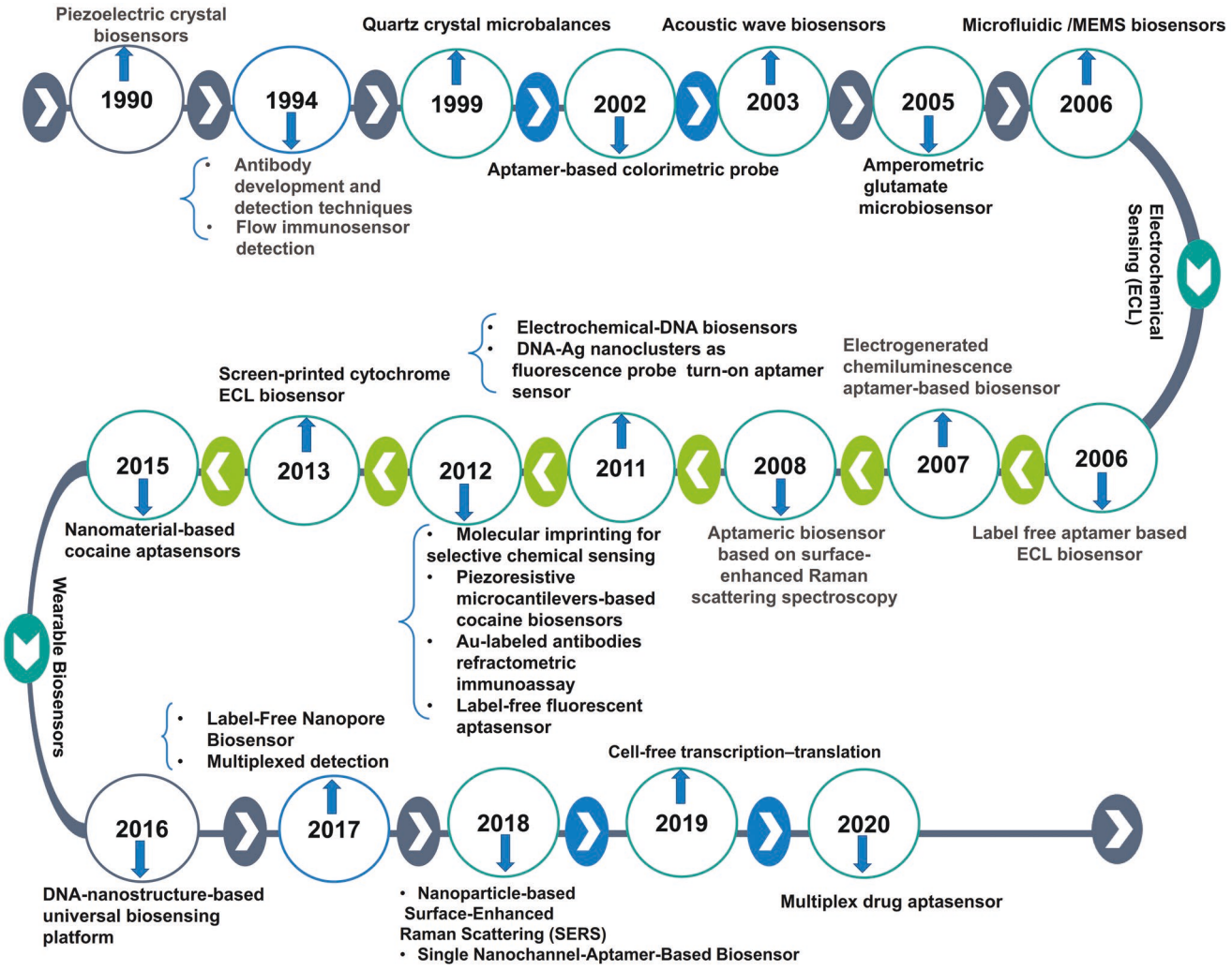

Figure 1. Timeline of the development of biosensors for the detection of abused drugs.

for multichannel and multiparameter recognition.[88] Optical biosensing can be based on bio-optrodes or evanescent field-based devices.

In bio-optrodes, the interplay between an analyte and a reagent immobilized on a fiber produces a measurable alteration in the optical properties of the fiber as a transductor. Optical evidence of this alteration can be done using dyes, fluorescent molecules, and bio- or chemiluminescent moieties.[89,90] Evanescent field-based biosensing devices use electromagnetic waveguides transmitting light under total internal reflection conditions, which creates an evanescent field. The field extends exponentially outside the waveguide at a specified distance from its surface, undergoing alteration with the receptor. Optical evanescent wave biosensing devices are popular due to the high intensity of the evanescent electromagnetic field and the high efficiency of recognition of the biochemical reactions occurring on the surface where the electromagnetic field is the strongest. This makes them highly sensitive and selective instruments for the analysis and identification of chemical or biological materials. They include fiber-optic devices, bio-optrode biosensors, SPR-based devices, SERS-based devices, total internal reflection fluorescence (TIRF) devices, optical waveguide interferometers, and ellipsometric and reflectometric interference spectroscopy (RlfS) biosensors.[91–93] **Table 2** lists recent studies in optical biosensors of abused drugs.[76,83,89,94–126]

2.1.3. Piezoelectric Sensors

Piezoelectric biosensors are based on electromechanical detection and are made of materials that respond to stress. Such sensors convert applied forces and mechanical strains into electrical signals. This signal is then amplified and displayed by an electronic circuit. These sensors have many applications in industrial fields

Table 1. Recent influential reports on electrochemical biosensors for abused drugs.

Biosensor type	Bioreceptor	Transducing procedure	LOD	Target molecules	Refs.
Electrochemical/cyclic voltammetry (CV)	Antibody	Functionalized screen-printed electrode (SPE) electrochemical biosensor with cobalt oxide nanoparticles and single-chain antibody	3.6 ng L^{-1}	Cocaine	[67]
Electrochemical/CV	Aptamer	Alternating current electroosmosis (ACEO) based capacitive sensing	7.8×10^{-15} M	Cocaine	[68]
Electrochemical/differential pulse voltammetry (DPV), CV and electrochemical impedance spectroscopy (EIS)	Antibody	Electrochemical sensing by an Au-cycteine modified sensor which was designed for dehydroepiandrosterone 3-sulfate (DHEA-S) detection	–	DHEA–S (codeine was used as interfing agant)	[69]
Electrochemical/CV and EIS	Aptamer	Polypeptide functional surface for the aptamer immobilization	1×10^{-9} M	Cocaine, benzoylecgonine	[70]
Electrochemical/CV	Aptamer	Electrochemical sensing by SWCNT/Au aptamer-CS-modified electrode	105×10^{-12} M	Cocaine	[71]
Electrochemical/CV	Aptamer	Biological nanopore embedded in a microchip	1×10^{-6} M	Cocaine	[72]
Electrochemical/ EIS	DNA	Faradaic impedance response (FIS) in reversible DNA nanostructure	0.21×10^{-9} M	Cocaine	[73]
Electrochemical/CV	Aptamer	Engineered aptamer-pendant DNA tetrahedral structure	33×10^{-9} M	Cocaine	[74]
Electrochemical/DPV	Aptamer	Enzyme-linked aptamer assay (ELAA)	20×10^{-9} M	Cocaine	[75]
Electrochemical/CV	Aptamer	Electrochemical, photoelectrochemical, and SPR using supramolecular aptamer complexes	1.0×10^{-6} M	Cocaine	[76]
Electrochemical/DPV	DNA	Graphene/AuNP nanocomposites	1×10^{-9} M	Cocaine	[77]
Electrochemical/EIS/CV/DPV	Aptamer	Electrochemical aptamer biosensors based on QDs	30×10^{-9} M	Cocaine	[78]
Electrochemical/DPV	Aptamer	AuNP-modified electrode	0.3×10^{-6} M	Cocaine	[79]
Electrochemical/DPV	Aptamer	Solid-state probe based electrochemical aptasensor	0.1×10^{-6} M	Cocaine and other drugs	[80]
Electrochemical/DPV	Aptamer	Electrochemical aptasensor based on Klenow fragment (KF) polymerase reaction	0.097×10^{-6} M	Cocaine	[81]
Electrochemical/square wave voltammetry (SWV)/CV	Aptamer	Incorporating modified gold nanoparticle	0.5×10^{-6} M	Cocaine	[82]
Electrochemical and fluorescence	Aptamer	Surface-enhanced Raman scattering spectroscopy	1×10^{-6} M	Cocaine	[83]
Electrochemical/SWV	Aptamer	Nanoporous gold-based electrochemical aptasensor	21×10^{-9} M	Cocaine	[84]
Electrochemical/microfluidic	Aptamer	Target-specific DNA aptamers fold to generate an electrochemical signal in the chip	–	Cocaine	[85]

as aerospace, nuclear, automotive, and most recently in medicine. However piezoelectric biosensors are still in their infancy and more research is needed before they will be commercialized.

Like other types of sensors, piezoelectric biosensors employ biological receptors such as antibodies, aptamers, enzymes, etc., for the detection of various analytes. For example, immobilization of antibody receptors on the surface of piezoelectric material makes an analytical immunosensor for application in biorecognition. Antigens/aptamers can be applied on the surface of piezoelectric materials as receptors to detect specific antibodies.[127–130] The use of antibodies also guarantees high selectivity due to their specific attachment to the target molecules or macromolecules.[131,132] Compared to electrochemical and optical biosensors, there has been less research on the development of a piezoelectric biosensor for the detection of abused drugs (see **Table 3**).[128–132]

2.1.4. Microfluidics Integrated Sensors

Recently, there has been significant progress in microfluidic integrated biosensor systems. Advances in microfluidics technology have enabled investigations of biological systems including biomolecules or organs and the development of state-of-the-art platforms such as LOC and organ-on-a-chip systems.[133] This emerging technology has added remarkable power to sensors due to the tiny volumes of samples required, leading to reductions in analyte and energy use, lowering costs, and bringing the ability to combine chemical and biological processes on a compact tool. Microfluidic devices have been employed in various fields such as biological screening and drug discovery, drug delivery,[133] POC devices for disease diagnosis, and environmental testing.[134]

Table 2. Recent studies on optical biosensors for abused drugs.

Biosensor type	Bioreceptor	Transducing procedure	LOD	Target molecules	Refs.
Optical/fluorescence	Split aptamer	Formation of nanocluster beacon sandwich, composed of DNA–silver nanoclusters	35×10^{-12} M	Cocaine and estradiol	[94]
Optical/fluorescence	Aptamer (MNS-4.1)	Fluorescence change induced by competitive binding cocaine	250×10^{-9} M	Cocaine	[95]
Optical/fluorescence	Aptamer	Aptamer-based folding fluorescent	$\approx 10 \times 10^{-6}$ M	Cocaine	[96]
Optical/fluorescence	Aptamer	Minor groove binder-based energy transfer (MBET)	0.2×10^{-6} M	Cocaine	[97]
Optical/fluorescence	Aptamer	Combining GO and Au nanoparticles (NPs)	0.1×10^{-6} M	Cocaine	[98]
Optical/fluorescence	Aptamer	Integrated signal transduction-based autonomous aptameric Machine	5×10^{-6} M	Cocaine	[99]
Optical/fluorescence	DNAzyme	Polymerization/nicking enzyme/DNAzyme cascade machinery	10^{-18} M	Cocaine	[100]
Optical/fluorescence	Aptamer	AuNPs and progressive dilution	2.1×10^{-6} M	Cocaine	[101]
Optical/fluorescence	Aptamer	Quantum-dot-based aptameric nanosensor fluorescence resonance energy transfer (FRET)	0.5×10^{-6} M	Cocaine	[76]
Optical/fluorescence	Aptamer	DNA–Ag nanoclusters as fluorescence probe for turn-on aptamer sensing	1×10^{-6} M	Cocaine	[102]
Optical/fluorescence	DNA strand	Strand-displacement polymerization and FRET	200×10^{-9} M	Cocaine	[103]
Optical/fluorescence	Aptamer	Signal Amplification through cycling exocleaving with a hairpin probe	1.76×10^{-9} M	Cocaine	[104]
Optical/fluorescence	Aptamer	Circular strand displacement amplification	190×10^{-9} M	Cocaine	[105]
Optical/fluorescence	DNA strand	Rolling circle amplification of DNA strand by magnetic beads	0.48×10^{-9} M	Cocaine	[106]
Optical/fluorescence	Excimer	Light switching excimer signaling approach	1×10^{-6} M	Cocaine	[107]
Optical/fluorescence	Aptamer	Strand displacement amplification	1×10^{-9} M	Cocaine	[108]
Optical/fluorescence	Aptamer	Fluorescent aptasensor–nanoparticle based on hairpin structure of excimer complementary strand	293×10^{-12} M	Cocaine	[109]
Optical/fluorescence	Aptamer	Label-free aptamer–fluorophore assembly	200×10^{-9} M	Cocaine	[110]
Optical/fluorescence	Aptamer	Aptamer–cocaine–aptamer complex on the surface of MoS_2@AuNPs was used to form a fluorescence signaling	0.54×10^{-12} M	Cocaine	[111]
Optical/fluorescence	–	Fluorescence quenching by Carbon-dot probe	7.24×10^{-6} M	Cocaine, nimetazepam, methamphetamine, heroin	[112]
Optical/fluorescence	–	Fluorescent fiber-optic chemical sensor based on a molecularly imprinted polymer	100×10^{-6} M	Cocaine	[113]
Optical/fluorescence	–	Fibre optic probe-based sensor based on molecular imprinted polymer	1×10^{-6} M	Cocaine	[114]
Optical/fluorescence	Aptamer	Microfluidic beads array fluorescent sensing by multienzyme-linked nanoparticle amplification and quantum dots labels	0.5×10^{-12} M	Cocaine, adenosine	[115]
Optical/fluorescence	Aptamer	Polarized optical microscopy	1×10^{-9} M	Cocaine	[116]
Optical/electrochemiluminescence (ECL)	Aptamer	Electrochemiluminescence "sandwich" biosensing	3.7×10^{-12} M	Cocaine	[117]
Optical/ECL	Aptamer	ECL aptamer-based (ECL-AB) biosensing	10×10^{-12} M[a)]	Cocaine and heroin	[118]
Optical/chemiluminescence	Aptamer	Chemiluminescence method using AuNPs	0.48×10^{-9} M	Cocaine	[119]
Optical/colorimetric or absorption spectroscopy	CTAB	Hybrid nanozyme peroxidase-like catalytic colorimetric sensor	128×10^{-9} M	Cocaine	[120]
Optical/absorption	Magnetic beads	Colorimetry/nanoplasmonic latent fingerprints	90 ng	Cocaine	[121]
Optical/absorption	Aptamer	Optical detection	100×10^{-6} M	Cocaine	[89]
Optical/absorption	Aptamer	Fast colorimetric sensing	50×10^{-6} M	Adenosine and cocaine	[122]
Optical/absorption	Aptamer	AuNPs and engineered DNA aptamers for colorimetry	2×10^{-6} M	Cocaine	[123]

Table 2. Continued.

Biosensor type	Bioreceptor	Transducing procedure	LOD	Target molecules	Refs.
Optical/absorption	Aptamer	Aptamer–gold nanoparticle with colorimetric image analysis android	15×10^{-6} M	Cocaine	[124]
Optical/Raman	Aptamer	Surface-enhanced Raman scattering spectroscopy	1×10^{-6} M	Cocaine	[83]
Optical/SPR	Antibody	Microarray chip-based SPR	1.4×10^{-9} M for heroin	Heroin and cocaine	[125]
Optical/fluorescence	Aptamer	Unmodified AuNPs is developed for aptamer-based fluorescence detection	80×10^{-6} M	Multiplex detection	[126]

[a]The indicated LOD value is for cocaine.

2.1.5. Electromechanical Sensors

Conventional micro and nanoelectromechanical systems (MEMS and NEMS) can be used for sensing, with the principle varying according to the type of target molecules, and the precision required.[135] The sensing mechanism is based on the alteration of the mechanical properties of the device such as capacitance modulation, piezo-resistance, and resonance frequency shift. Atomic force microscopy (AFM) cantilevers, as elementary MEMS devices, have been introduced as earlier versions of electromechanical-based biosensors.[136] In this method, the silicon cantilever of a few micrometers which has intrinsic flexibility can bend and detect microsized compounds and particles. This technology is multifunctional, nondestructive, very precise, and a real-time method useful for a wide range of applications, such as plastic explosive gas biosensors, microorganism detection as part of liquid biosensors, and genomics and proteomics.[137] This technique may not be suitable for the detection of abused drugs as they are in the nanometre size range and most AFM devices cannot detect molecular-sized particles. However, detection of abused drugs, e.g., heroin and cocaine, has been reported by other electromechanical biosensors such as quartz crystal microbalance (QCM) sensors.[138] One of the major drawbacks of this method is that detection is usually limited to volatile compounds or to the compounds that can be evaporated and exist in the gaseous phase.

3. Abuse Drug Sensing

3.1. Cocaine Sensing

Cocaine is one of the most commonly abused drugs and can have toxic effects on the cardiovascular, respiratory, and central nervous systems.[139–142] In 2017, the European Monitoring Centre for Drugs and Drug Addiction (EMCDDA) reported that cocaine ranked second in terms of drug usage in 2016, with 3.5 million consumers in the 15–64 age groups (1% of the population). In young adults (15–34 years old), 2.3 million individuals were found (1.9% of the population).[143]

Different types of agents including biomolecules such as DNA, enzymes, and antibodies as well as nanoprobes such as Au nanoparticles, carbon nanotubes, have been utilized in biosensors to detect cocaine. Since cocaine is a small molecule, aptamers are more suitable for cocaine detection. Cocaine tends to be positively charged due to the presence of amine groups, hence it tends to bind with negatively charged sites.[96] Generally, the interaction between aptamer and cocaine involves an unfolding–folding mechanism. The three-way junction formation of the aptamer only occurs in the presence of cocaine. Aptamers have been engineered to tune their affinity to cocaine and to improve signal transduction. Swensen et al.[85] developed a microfluidic electrochemical aptamer-based sensor (MECAS) chip. By integration of target-specific DNA aptamers, cocaine could be detected in undiluted blood serum allowing continuous and real-time (≈1 min time resolution) monitoring of cocaine at low micromolar concentrations. They proposed the integration of folding-based electrochemical sensors with miniaturized detection systems as POC diagnostic tools, which allow for real-time detection of a vast range of molecular targets. In the presence of methylene blue (MB) which acts as a redox agent and the modifier of unfolded aptamer, the cocaine binding signal is obtained from the folded mechanism and charge transfer from MB to the electrode.

An aptamer-based microfluidic array biosensor based on amplifying nanoparticles was utilized by Zhang et al. to detect cocaine and adenosine.[115] Using a dual signal amplification

Table 3. Recent studies on piezoelectric biosensors for drugs of abuse.

Biosensor Type	Bioreceptor	Transducing procedure	LOD	Target molecules	Refs.
Piezoelectric /electromagnetic piezoelectric acoustic sensor (EMPAS)	Aptamer	quartz substrate functionalized with linker and anti-cocaine MN4 DNA aptamer	0.9×10^{-6} M	Cocaine	[128]
Piezoresistive microcantilevers	Aptamer	A Wheatstone bridge composed of four aptamers coated microcantilevers for signal harvesting	1 ng mL^{-1} M	Cocaine	[129]
Microcantilever	Aptamer	Aptamer functionalized microcantilever colorimetry sensing	5×10^{-6} M	Cocaine	[130]
Piezoelectric affinity sensors	Antibody	formation of affinity complexes between an immobilized cocaine derivative and an anti-cocaine antibody	100×10^{-12} M	Cocaine cholinesterase	[131]
Piezoelectric	Antibody	piezoelectric immunochemical sensor	–	Cocaine, parathion	[132]

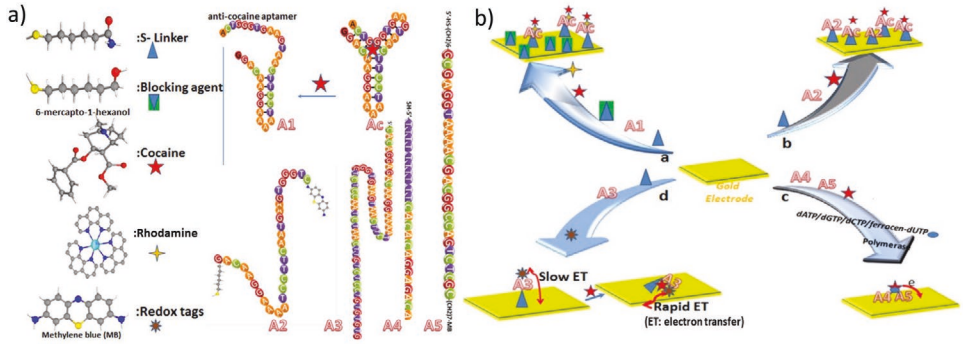

Figure 2. Schematic representation of the main aptameric electrochemical biosensing methods for cocaine detection based on a gold electrode. The nanoarchitectonics of gold for electrochemical and ECL biosensing of cocaine. The four most common pathways are represented. The main elements including various aptamer/tag combinations (A1 and A3: cocaine aptamers; A2, A4, and A5: cocaine aptamers combined with s-linker and methylene blue; Ac: aptamer–cocaine complex), Sulfurized linking molecule for attachment of aptamer to the gold substrate (S-Linker), Blocking agent for deactivating s-linkers that are not bonded to aptamers, optically active molecules such as rhodamine and electrochemically active molecules (redox-tags) such as MB are represented. The boosting of electron transfer (ET) on the surface of gold with aptamer-analyte, e.g., cocaine, redox complex shapes, is shown.

approach, the designed microfluidic biosensor could discriminate as little as 0.1×10^{-12} M of adenosine and 0.5×10^{-12} M of cocaine, a 500-fold increase in detection limits. They confirmed that the microfluidic-based technique was a fast and effective system, suitable for aptamer-based targets tests, and required only minimal (microliter) reagent usage. Their strategy is based on a combination of electron-rich protein functionalized microbead and cocaine aptamer as a sensing element and horseradish peroxidase (HRP) functionalized gold nanoparticles (Au NPs) as labels. In the proposed detection mechanism, the cocaine binds with aptamer forming a complex structure that reduces the number of conjugates of aptamer-AuNPs-HRP. The residual conjugates actively catalyze the formation of tyramine radicals from biotin-tyramines. The reaction between the radical and the residue proteins on the microbeads induces the covalent attachment of biotin moieties. These moieties can produce a fluorescence signal in the presence of streptavidin-conjugated quantum dots. Since the residual conjugates on the surface of the microbead depend on the number of cocaine molecules, the fluorescence signal indirectly depends on the cocaine concentration. Similarly, Zhang et al.[144] designed a reusable electrochemical biosensor based on a structure-switching hairpin probe to detect small molecules, using cocaine as a model analyte. They used alternating current (AC) voltammetry to identify cocaine in a linear dynamic range from 1×10^{-9} to 1000×10^{-9} M with a low detection limit of 0.7×10^{-9} M. The authors asserted that they could simply regenerate the biosensor via hot water melting. A different aptamer-based electrochemical biosensor, an ELAA, was fabricated by Zhang et al. for detecting cocaine through aptamer fragment/cocaine conformation. Like other reports, two subunits of the cocaine aptamer were modified. One was modified with thiol groups to bind with Au surface, and the other one was modified with biotin. The electrochemical signal was obtained from the complex structure of cocaine-aptamer and the streptavidin horseradish peroxide label that supports the redox reaction of hydroquinone in the presence of H_2O_2. Due to the affinity of aptamer fragments with cocaine,[75] DPV signal alteration allowed detection of cocaine ranging dynamically from 0.1×10^{-6} to 50×10^{-6} M and the detection limit was 20×10^{-9} M (signal-to-noise ratio: S/N = 3). This aptasensor had low background current and high sensitivity.

There are various reports of aptameric electrochemical detection of cocaine using gold electrodes. **Figure 2**a schematically shows the main aptamers and protocols employed. As illustrated the applicable and effective nanoarchitectures are based on nanoenabled gold electrodes. On the surface of gold electrodes, e.g., Au NPs, the physical or chemical assembly of target-specific linkers and receptors, i.e., aptamers, provides the capability to respond to the target molecules or germs. The implementation of appropriate optical tags and electroactive probes may improve the sensitivity of the proposed biosensor through integrating optical-electrochemical sensing. Figure 2b outlines the main biosensing approaches that have been developed based on gold electrodes and aptamers.

An ECL mechanism for the identification of cocaine by aptamer probes was developed by Zhao et al.[145] The ECL technique is direct, label-free, specific, and sensitive with a LOD of 0.2×10^{-12} M for cocaine. The observed duplex formation in an aptamer was utilized for intercalating a $Ru(phen)_3^{+2}$ probe to detect cocaine by ECL (**Figure 3**). Initially, immobilization of the anti-cocaine aptamer was performed on a gold electrode through a gold–thiol bond (Figure 3). The connection of cocaine with its aptamer led to the creation of the duplex. Next, the $Ru(phen)_3^{+2}$ probe underwent intercalation into the duplex. Upon applying a fixed potential to the modified electrode, ECL emission was observed proportional to cocaine concentrations. Sun et al.[118] found a binding constant of $4.6 \pm 0.3 \times 10^{-9}$ M between cocaine and its aptamer, while another study showed a dissociation constant of 0.2×10^{-6} M.[146]

Semiconductive QDs like Au QDs are effective substrates for nanoarchitecting drug biosensors. QDs possess high stability and engineered morphology, narrower and tunable emission as well as high quantum yields. These exclusive features make QDs very applicable for the design and development of biosensors especially when an electrochemical-optical signaling method is implemented. An electrochemical-optical scaffold was designed by Freeman et al. using an aptamer to detect cocaine.[147] They proposed supramolecular self-assembly of aptamer segments using QD-based FRET excimer-based optical sensors and surface-restricted electrochemical sensors. In their QD-based FRET cocaine sensor, two modified subunits of an

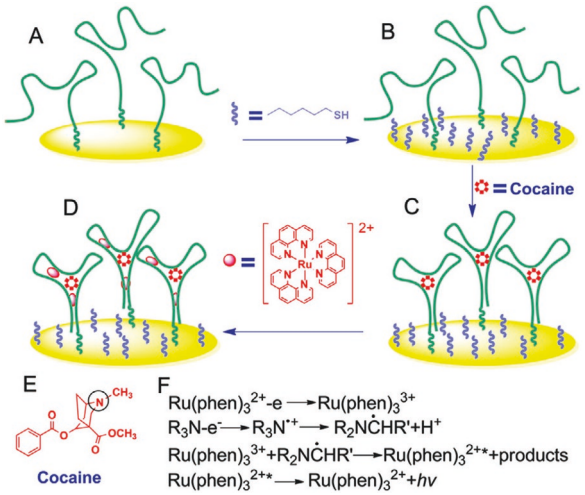

Figure 3. Schematic diagram of the label-free aptasensor with the analyte-induced formation of duplex sections for probe intercalation. A) Self-assembly immobilization of the anti-cocaine aptamer on the gold electrode; B) blocking of the active site with 6-mercapto-1-hexanol; C) cocaine-induced formation of the duplexes; D) intercalation of $Ru(phen)_3^{+2}$ into the formed double strand sections. E) The molecular structure of cocaine. F) The $Ru(phen)_3^{+2}$ ECL excitation mechanism of cocaine as a tertiary amine-containing molecule. Adapted with permission.[145] Copyright 2011, Royal Society of Chemistry.

anti-cocaine aptamer were used. The first subunit was connected to CdSe/ZnS QDs while the second subunit was connected to the Atto 590-dye molecule. The FRET phenomenon between the donor of QDs and the acceptor of dye was supported by the formation of cocaine-aptamer supramolecular structures. The phenomenon is not observed in the absence of cocaine indicating the effectiveness of FRET-based cocaine sensor with LOD of 1×10^{-6} M. Furthermore, in their proposed sensor, the thiolate subunit aptamer was assembled on the gold surface and the redox label of MB modified the other subunit of the aptamer. In the presence of cocaine, a cocaine-aptamer supramolecular structure is formed along with the redox reaction of MB resulting in the electrochemical signal. This system has a detection limit of 10×10^{-6} M, 10 times higher than that of the optical system. This elegant procedure was originally developed by Stojanovic et al.,[148] who designed optimal sequences of aptamer segments for self-assembly of supramolecular analyte–nucleic acid structures, resulting in fluorescence quenching of the dye-labeled aptamer segments. Self-assembly of dye-functionalized nucleic acids composed of optimized sequences of cocaine aptamer in the presence of analyte, i.e., cocaine, enables the core biosensing nanoarchitectonics for trace biosensing of drugs. Freeman et al. demonstrated that the creation of the supramolecular aptamer–substrate complex could allosterically stabilize the creation of the secondary excimer supramolecular complex. The 39-mer cocaine-binding aptamer was designed to be separated into two subunits, C1 and C2. The C1 subunit was labeled with 5(6)-carboxy-fluorescein fluorophore (6-FAM) while the C2 subunit was labeled with a 3'-dabcyl quencher. The self-assembly of F-C1 and C2-D in the presence of cocaine functioned well as a fluorescent cocaine sensor with a detection range of 10–1250 $\times 10^{-6}$ M.

An aptamer-modified electrochemical electrode as a framework for cocaine biosensing was developed by White et al.[149] The team systematically investigated the impact of probe (aptamer) packing density, the AC frequency applied for interrogating the sensor, and the nature of the self-assembled monolayer (SAM) utilized for passivation of the electrode on the functionality of electrochemical-aptamer based (E-AB) sensors for small molecules, e.g., cocaine, and proteins, e.g., thrombin. Control of aptamer concentration enabled them to regulate the density of probe DNA molecules on the electrode surface, over an order of magnitude. Bozokalfa et al. reported the construction of an aptasensor platform on polythiophene containing polyalanine homopeptide side chains (PT-Pala) by an electrochemical coating of the surface of an electrode followed by attaching a cocaine aptamer to the polymer through covalent conjugation chemistry.[70] A label-free detection mechanism is proposed based on the prevention of the charge transfer of redox probe of $[Fe(CN)6]^{3-/4-}$ to the electrode surface due to the formation of a three-way junction of the cocaine–aptamer complex structure. This technique is a simpler method since no redox label is required. This system detected cocaine and its metabolite, benzoylecgonine (BE), in the linear range from 2.5×10^{-9}–10×10^{-9} M and 0.5–50 $\times 10^{-6}$ M for cocaine and BE, respectively. Moreover, this aptasensor also measured BE in synthetic urine and saliva with recoveries of 94.8% ± 8.8% and 94.61% ± 3.24% respectively. The covalent attachment of an aptamer on the surface of functionalized or coated nanoelectrodes ,e.g., Au or Pt nanoparticles, provides a durable and robust nanoarchitectonics for cocaine biosensing. However, in comparison with the aptamer self-assembly procedure, the covalent attachment procedure provides lower throughput and sensitivity. Baker et al.[150] manufactured an electrochemical aptamer-based biosensor by designing an E-AB sensor to detect cocaine electrochemically (**Figure 4**). The fabrication is based on the self-assembly of MB-tagged aptamer on a ≈1 mm^2 gold electrode through an alkanethiol group. The authors claimed that this strategy can detect 500 µM of cocaine in human saliva in a second and can detect the molecule in the presence of a masking agent.

Electroactive tags such as organometallic complexes or their combinations with aptamers are one of the main elements of ECL nanoarchitectonics. Immobilization of these ECL tags may happen through a direct strategy or after attachment to

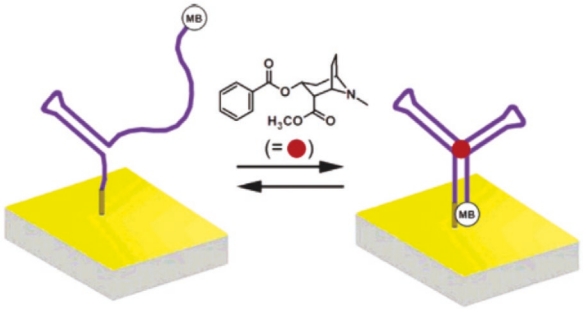

Figure 4. Schematics of the E-AB cocaine biosensor. Modified aptamers where MB redox tags are covalently attached via a seven-carbon linker to the termini, or an internal thymidine, as indicated. Reproduced with permission.[150] Copyright 2006, American Chemical Society.

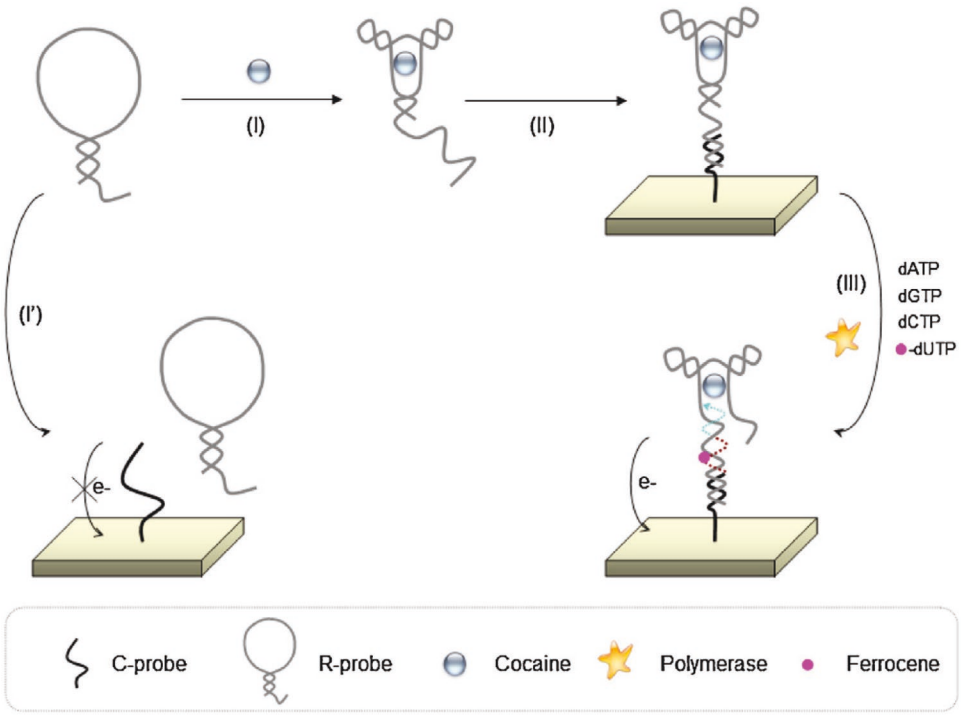

Figure 5. Schematic illustration of the electrochemical aptasensor nanoarchitecture based on the polymerase extension reaction. The strategy includes: (I) Binding of the aptamer and cocaine in sample solution; (II) capture of the aptamer-cocaine complex on the gold electrode; and (III) polymerase extension reaction in the presence of dATPs, dGTPs, dCTPs, Fc-dUTPs, and KF polymerase. (I') The R-probe keeps its hairpin conformation without cocaine, and with minimal hybridization with the C-probe. Reproduced with permission.[81] Copyright 2011, Elsevier.

appropriate nano-supports like silica nanoparticles. The capture probe, an aptamer with a hexanethiol group, was immobilized on a gold electrode through thiol-gold coupling, and the other aptamer (the detecting probe) was tagged with the ECL reagent tris(2,2'-bipyridyl)ruthenium(II)-doped silica nanoparticles. Another aptamer-based ECL biosensor was made by Cai et al.[117] to detect cocaine on banknotes. A sandwich biosensor was proposed since an aptamer alone was capable of bisecting into two segments and the two separated sections create a folded, combined complex in the presence of targets. A segment with hexane-thiol was utilized to bind with the gold surface and the other one was modified by an ECL label of tris(2,2'-bipyridyl) ruthenium(II)-doped silica nanoparticles (RuSiNPs). In the presence of cocaine, the self-assembly of the cocaine-aptamer complex allows the RuSiNPs to be immobilized on the surface electrode and generate an ECL signal. The improved ECL intensity was proportional to the logarithm of cocaine concentration ranging between 1.0×10^{-9} and 1.0×10^{-11} M, with a detection limit of 3.7×10^{-12} M. The proposed strategy for boosting the ECL signal is very promising in comparison with conventional electroactive tags where the electron-transfer (ET) process through the redox reaction is slow. In contrast by employing nano-architected electrochemical probes ,e.g., RuSiNPs, the ET phenomenon improves, and signal throughput is enhanced which results in low LODs.

Among the various ECL tags applied in cocaine biosensors, ferrocene (Fc) is one the most frequently used as it offers high signal throughputs. In addition, Fc could be easily coupled with nucleic acids for specific purposes. He et al. designed a cocaine electrochemical aptasensor using a KF polymerase reaction combined with aggregation of the ferrocene-functionalized oligonucleotide.[81] Their detection system involves a recognition probe (R-probe) containing a cocaine aptamer, a capture probe (C-probe) modified gold electrode, an Fc labeled aptamer (Fc-dUTP), and a KF polymerase agent. The cocaine reacts with the R-probe in the nucleotide solution before being deposited on the electrode. In the solution, the R-probe forms a complex structure with cocaine by changing its hairpin conformation into a tripartite complex. The complex then binds with C-probe, with the support of KF polymerase, forming a longer DNA strand that is complementary to the R-probe. The electrochemical signal is obtained when Fc-dUTP is incorporated during polymerization. The biosensing procedure (**Figure 5**) included the creation of a cocaine–aptamer complex, capture of the complex on the electrode, and the polymerase extension of the capture probe with the detection probe serving as a template. This method of detecting cocaine results in a very low background signal and considerable signal improvement of up to ninefold after adding analyte. It allows the identification of cocaine in the range of 200 nm–5 µm with a detection limit of 97×10^{-9} M. The reported detection limit is outstanding indicating the efficacy of the proposed biosensor nanoarchitecture.

Other types of electrochemical probes such as inorganic redox complexes, e.g., $[Fe(CN)_6]^{3-/4-}$ have been used in the development of cocaine biosensors. These redox probes are mainly used in the voltammetry method of detection and provide straightforward label-free biosensing tools when combined with aptamer capture tags immobilized on nanoenabled supports such as Au NPs and QDs. Hua et al. proposed a label-free electrochemical nucleic acid aptasensor for cocaine by immobilizing

thiolated self-assembled DNA sequences on a gold nanoparticle-modified electrode.[79] Once cocaine forms a specific complex with the aptamer, the conformation of the nucleic acid aptamer shifts to a locked structure leading to an altered biosensor interface and a disparity in the equivalent peak current of an electrochemical probe ($[Fe(CN)_6]^{3-}/^{4-}$). Cyclic voltammetry (CV) and EIS were used to characterize the modified cocaine electrode. The reduction in the peak current response of the aptasensor was linear in a cocaine concentration in the range of 1.0×10^{-6}–1.5×10^{-4} M with a LOD of 3×10^{-7} M at 3σ. Subsequently, a new electrochemical cocaine aptamer biosensor based on CdS QDs as the immobilized substrate was designed, which utilized the sulfur–sulfur affinity, increasing binding between heavy metal ion of quantum dots and sulfhydryl group of aptamer.[78] Different concentrations of cocaine result in different degrees of structure switching of aptamer from hairpin structure to tripartite complex structure. The linear range was between 1×10^{-9} M and 1×10^{-6} M with a correlation coefficient of 0.9765 using $[Ru(NH_3)_6]^{3+}$ as a probe, and 1×10^{-7}–1×10^{-6} M with a correlation coefficient of 0.9839 using $[Fe(CN)_6]^{3-/4-}$ as a probe. It appears that this electrochemical aptasensor using a cationic probe, responds better than an anionic probe due to the negatively charged nature of the phosphate-based cocaine aptamer. Moreover, cocaine detection in human serum with this technique had a high recovery of >95%.

In drug biosensor nanoarchitecture the position and arrangement of all building blocks, i.e., substrate, capture probes, electrochemical probes, and optical tags, are important factors determining the analytical efficiency of the biosensor. Meanwhile, the position of the electrochemical probe is crucial because the distance between this probe and electrode surface directly affects the electron transfer phenomenon and the obtained analytical current. Li et al. employed surface-restricted DNA structures with suitable redox labels to monitor target-stimulated structural shifting of DNA or aptamer-specific small molecule probes by measurement of electrochemical currents proportional to the distance between the redox label and the electrode surface. These researchers observed that sensing functionality improved significantly by optimizing the DNA self-assembly procedure at electrode surfaces or by introducing nanomaterial-based signal augmentation.[151] The proposed E-AB biosensors require recalibration for accurate molecular measurement. A "dual-frequency" method was developed by Li et al. for calibration-free electrochemical biosensors, using SWV to monitor binding-stimulated variations in electron transfer kinetics. **Figure 6** shows the principles of their E-AB biosensor.[152] In the presence of cocaine, the change in conformational aptamer induces electron transfer between the MB label and the electrode. The free calibration in small molecule detection operation via ratiometric output is independent of the unit, sensor to sensor fabrication, and degradation of the sensor itself.

Engineering the nanoarchitectonics of aptamers on the gold electrode surface is required for the development of marketable aptasensors and tackling the current drawbacks in the field. For example, using carbon nanotubes aptamers on the gold surface could be assembled. Taghdisi et al. designed an electrochemical aptasensor to identify cocaine with a gold electrode, single-wall carbon nanotubes (SWNTs), and a complementary strand of aptamer with high affinity.[153] Unlike other detection mechanisms that utilize a signal change due to cocaine-aptamer deposition on the electrode surface, the signal was generated due to the release of the complex from the surface. Before aptamer–cocaine conjugation, the aptamer weakly binds with its complementary strand (CS) and a few SWNTs can bind to the CS resulting in a weak electrochemical signal. In the presence of cocaine, the strong interaction between cocaine and aptamer causes the aptamer to release from the CS leaving the CS as an ssDNA. Since SWNTs have a high affinity to the CS, the SWNTs couple with the CS of the aptamer-modified electrode, which generates a robust electrochemical signal. Their electrochemical aptasensor is selective for cocaine with an LOD as little as 105×10^{-12} M. Furthermore, the system had a LOD of 136×10^{-12} M for the detection of cocaine in serum. The reported detection limits indicate that incorporating carbon nanotubes into the nanoarchitecture of drug biosensors improves the sensitivity.

An alternative strategy for improving the nanoarchitectonics of the aptamers-electrode system in drug biosensing is modifying the surface of the electrode by increasing its intrinsic affinity, porosity, and other physicochemical properties. Tavakkoli et al. designed a nanoporous gold-based electrochemical aptasensor to detect cocaine[84] through immobilization of the 5-disulfide-functionalized end of an aptamer sequence on a nanoporous gold (NPG) electrode, after which its 3-amino-functionalized end was conjugated to 2,5-dihydroxybenzoic acid (DHBA) as the redox probe. When cocaine is present, the aptamer goes through a configurational alteration from an open unfolded state to a closed configuration, thereby reducing the distance between DHBA and the electrode surface, leading to improved electron transfer. Using a square wave voltammetric technique optimized for two linear response ranges, concentrations of cocaine were measured for 0.05–1 and 1–35 $\times 10^{-6}$ M, with an LOD of 21×10^{-9} M.

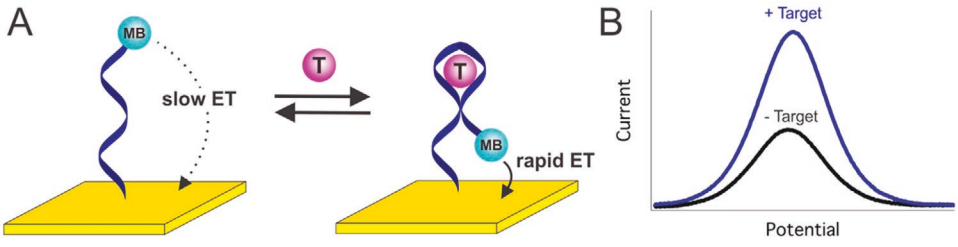

Figure 6. E-AB biosensors. A) E-AB sensors are comprised of an electrode-bound, redox reporter-modified aptamer that undergoes a binding-induced conformational change which results in rapid electron transfer and improved current signal B) target-dependent change in current. Reproduced with permission.[152] Copyright 2017, American Chemical Society.

Xia et al. produced label-free, dual-analyte electrochemical biosensors as a molecular-electronic logic gate.[154] Their two-analyte exclusive OR (XOR) logic instrument could determine the concentrations of both cocaine and a complementary DNA (cDNA) target as inputs and produce changes in faradaic current from the connected redox reporter as the output. Cocaine at a level of $>250 \times 10^{-6}$ M was applied as the input, the logic gates translated molecular (concentration) signals into electrical signals and induced a warning alarm if cocaine concentrations exceeded a predetermined limit (1×10^{-6} M). In this logic gate, they utilized the electrochemical cocaine biosensor of earlier studies.[150]

Employing complementary probes labeled with optical or electrochemical tags is a strategy for the development of biosensors nanoarchitectonics based on the self-assembly of aptamers and their complementary sequences. The proposed method offers the advantage of effective labeling of the electrode surface and enhancing electron transfer and the final signal. Yang and Zhang introduced an accessory probe into the sensor structure to improve the sensitivity.[155] The proposed signal-on biosensor comprises a thiol functionalized capture probe fixed on the gold electrode surface, an electrochemical MB-modified reporter probe, which is complementary to the capture probe, and an adjunct probe fixed close to the capture probe. The adjunct probe serves as a fixing agent to immobilize the component of the reporter probe displaced by the target DNA or protein. This increases the probability of the dissociation of the reporter probe for collision with the electrode surface and electron transfer. The sensitivity of a biosensor with an accessory probe improves for a wide dynamic range for DNA and thrombin assays, as it can distinguish a one-base incompatible target DNA. This biosensor can be reused repeatedly and can precisely detect many biomolecules, such as RNA, proteins, and small molecules, such as cocaine.

Responsive materials and smart molecules can introduce remarkable improvements in the nanoarchitectonics of drug biosensors. Zhang et al. designed a multiple-use electrochemical aptasensor to detect small molecules with a structure-switching hairpin probe.[144] Upon the addition of target molecules, such as cocaine, the target molecule, and the signal probe compete with the aptamer probe, thereby inducing the signal probe to change from a stretched duplex to a hairpin structure. Measurement with AC voltammetry provides sensitive detection of cocaine in a linear dynamic range between 1×10^{-9} M and 1000×10^{-9} M with a low detection limit of 0.7×10^{-9} M. It is possible to regenerate the biosensor simply with hot-water melting to make a multiple-use device. The obtained analytical parameters demonstrate how biosensing techniques can be improved through the effective application of functional and responsive materials and molecules. The structure switching of employed probes or other types of responsive proves not only improves the selectivity of the biosensor for targeting small molecules such as cocaine, but also increases the sensitivity and current density by boosting the electron transfer process. This is mainly due to decreasing the distance between the electrode surface and probe after combining to the target molecule, e.g., cocaine, and successive structure switching.

Considering the structure switching property of the electrochemical probes the altered configuration of the employed probes may induce orderliness in their arrangement on the electrode surface. In fact, the folding and coiling of the probes after their attachment to the target molecule optimizes the biosensor nanoarchitecture by decreasing the intrinsic randomness of the initial self-assembly phenomenon of aptamers. Li et al. manufactured an E-AB to detect drugs with a cocaine-coupling aptamer by self-assembling a $Ru(bpy)_2(dcbpy)NHS$-labeled aptamer and immobilizing it on a gold electrode surface via thiol-Au bonds.[156] The improved cocaine detection was ascribed to an alteration in the configuration of the electrochemical probe from a random coil-like conformation to a three-way junction structure, which came in closer proximity to the sensor surface. The combined electrochemical intensity was linear for cocaine concentrations ranging between 5.0×10^{-9} and 3.0×10^{-7} M, with a LOD of 1.0×10^{-9} M. The nanomolar detection limit for this biosensor shows the effectiveness of using electrochemical probes with switching-structure and dual-configuration properties.

For manufacturing high-throughput optical drug biosensors, introducing cluster nanoarchitectonics through agglomeration and self-assembly of nanoparticles such as Au, Ag would be advantageous especially when the fluorescence yield of probes is important. Following this strategy, Zhou et al. used DNA-Ag nanoclusters (NCs) as a fluorescence probe for a turn-on aptamer sensor of small molecules including cocaine.[102] Their findings revealed that the two aptamer segments coupled with cocaine, in turn, reached the two G-rich sequence segments on the probe and improved significantly the fluorescent intensity of DNA-Ag NCs. This cost-efficient turn-on fluorescent cocaine sensor had an LOD of 0.1×10^{-6} M. An aptamer-based fluorescence biosensor was proposed by Luo et al. for the multimodal detection of adenosine, thrombin, and cocaine, using AuNPs.[126] The biosensor's principle is depicted in **Figure 7**.

Another sensitive fluorescence biosensor based on aptamer and rolling circle amplification for cocaine detection was developed by Ma et al.[106] They immobilized cocaine aptamers onto Au nanoparticles modified magnetic beads hybridized with short DNA strands. In the presence of cocaine, the short DNA strand was displaced from the aptamer due to cocaine binding with aptamer. Next, the short DNA strand was separated by magnetic beads and used to originate rolling circle amplification (RCA) as a primer. The end products of rolling circle amplification were detected by fluorescence signal generation upon molecular beacons hybridization (**Figure 8**). This method reduced the background signal and was able to detect as low as 0.48×10^{-9} M cocaine.

Another important aspect of the reported drug biosensors nanoarchitectonics is immobilizing a combination of different nanoparticles for a multiplex and multimodal sensing system. As an important study in this regard, Man et al. constructed a multimodal biomolecular recognition device using photo-stimulated improved Raman spectroscopy (PIERS) mechanism.[157] In the PIERS sensor, the target molecule triggered TiO_2@AgNP substrate coupling with Raman tag-labeled gold nanoparticles probes, leading to the formation of sandwich complexes. Pre-irradiation with ultraviolet induces the formation of oxygen vacancy defect states near the TiO_2 conduction band. The electrons from the states are then excited and migrated to AgNPs by Raman laser irradiation. The PIERS effect on the AgNP and AuNP depends on the amount of cocaine attached by the aptamer. The PIERS sensor can operate as a multipurpose recognition scaffold for sensitive analysis of diverse biomolecules, such as small molecules and drugs (cocaine, LOD of 5×10^{-9} M). The reported biosensor

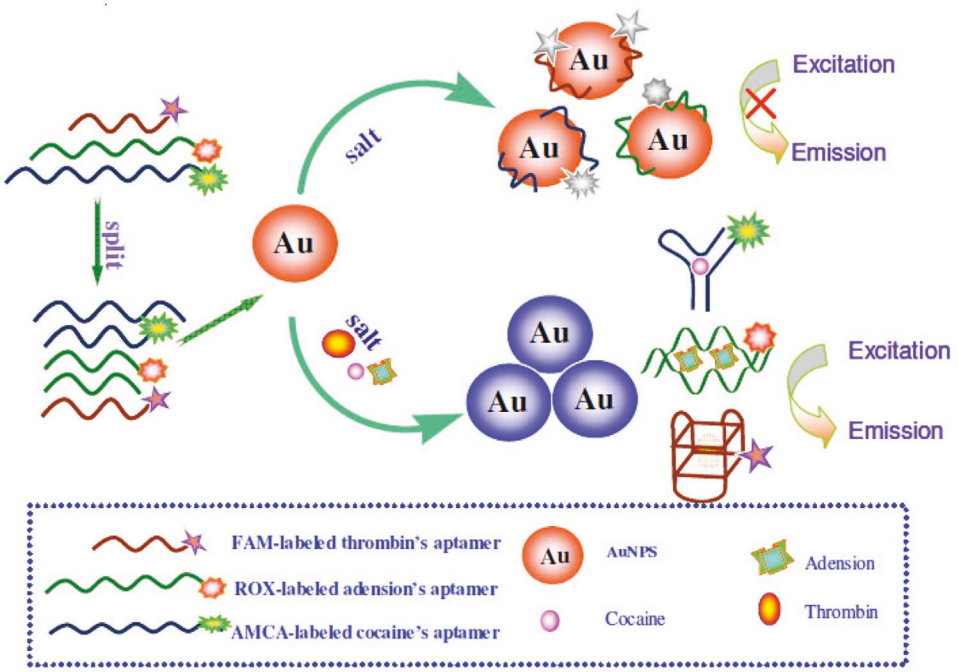

Figure 7. An aptamer-based fluorescence biosensor for multiplex detection using unmodified AuNPs to detect adenosine, thrombin, cocaine, and other small molecule substances. Adapted with permission.[126] Copyright 2012, Royal Society of Chemistry.

parameters indicate the effectiveness of the multimodal approach in the design and development of drug biosensors.

In developing optical biosensors for drug recognition and other sensing purposes, using fluorescence quenching signals has proven to be a simple and very selective approach. Tang reported a multiple-use split-aptamer-based biosensor to detect cocaine rapidly in serum utilizing an all-fiber vanishing wave optical biosensing setup.[158] The presence of cocaine led to the quick formation of a tripartite intersection by both fragments of the cocaine aptamer, and effective quenching of the fluorophore group of one fragment occurred by the quenching group of the other fragment. cDNA sequences immobilized on the optical fiber biosensor hybridize the tail of the tripartite intersection. Excitation of fluorescence was done with an evanescent wave, and the fluorescence signal was proportional to cocaine concentrations. Cocaine was detected in 450 s (300 s for incubation and 150 s for recognition and reconstruction) with a LOD of 165.2×10^{-9} M. Toppozada et al.[159] conducted a study on a fiber optic immunosensor for quantitating cocaine in coca leaf extracts. A monoclonal antibody (mAb) against benzoylecgonine (BE), the main metabolite of cocaine, was covalently immobilized on quartz fibers and utilized as the biological sensing agent in a transferrable fluorometer. After coupling with the fiber, benzoylecgonine-fluorescein (BE-FL) was employed as the optical signal maker. Cocaine competes for the mAb and interferes with the coupling of BE-FL, resulting in reduced fluorescence transferred by the fiber. Wang et al. employed a polarized optical microscope for sensing cocaine by utilizing the configurational alterations of an aptamer at the water/liquid crystal interface.[116]

Liquid crystals (LCs) are an attractive class of organic materials that can transduce and amplify a molecular stimulus into optical signals thanks to their elastic and birefringence properties. Wu's group[116] developed an aptamer-based LC sensor for cocaine. Detection was done using 3-morpholinopropanesulfonic acid with an amphipathic structure at a water/LC interface to recognize cocaine. The cocaine aptamer coupling occurs at the interface. An alteration in the configuration of the aptamer upon coupling cocaine triggers the attached LCs to shift from the homeotropic to the planar phase. Thus, a polarized optical microscope can detect coupling. The coupling of cocaine results in the change in the configuration of aptamer from a hairpin structure to a three-way junction structure, which is confirmed by fluorescence spectroscopy and circular dichroism signal. This specific test can measure a cocaine concentration of 1×10^{-9} M–10×10^{-6} M with a detection limit of 1×10^{-9} M. This LC-based sensor can also detect cocaine in urine.

Wenger et al.[160] manufactured an optical cocaine biosensor using refractometry and used a combined scaffold to detect cocaine with high sensitivity, as shown in **Figure 9**a,b. In this work, they used Au-labeled antibodies to enhance selectivity. A waveguide grating functionalized with a cocaine multivalent antigen-carrier protein conjugate is used. In the immunoassay system, cocaine-specific antibodies bind competitively to the immobilized conjugates. The use of gold conjugated monoclonal antibodies in place of free antibodies results in a 1000-fold increase in the sensor sensitivity, with cocaine in a liquid sample being detectable down to a concentration of 0.7×10^{-9} M within 1 min. This LOD was lower using a longer time (0.2×10^{-9} M after 15 min), making the system suitable for detecting narcotic drugs at airport security control points. Figure 9b,c displays the aptasensing mechanism. Wu et al.[107] developed a generalized technique for tailoring aptamer sequences into practical subunits for target-stimulated light switching excimer sensors. They bisected a single-strand aptamer into two segments and tagged their terminals with a

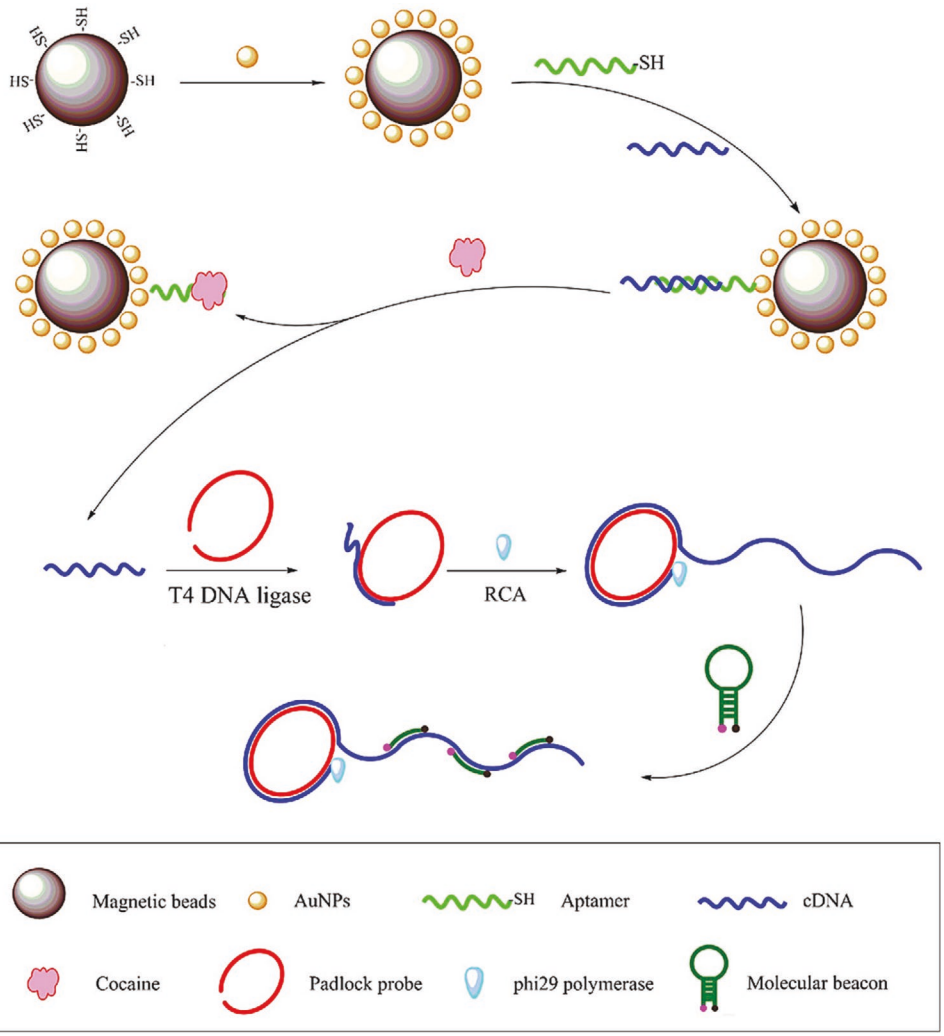

Figure 8. Schematic outline of fluorescence biosensor to detect cocaine based on signal amplification under RCA and separation by magnetic beads reducing the background signal. Reproduced with permission.[106] Copyright 2011, Elsevier.

pyrene molecule while simultaneously maintained their coupling affinity to target molecules (**Figure 10**).

Like electrochemical biosensors, inhibiting AuNPs aggregation throughout the self-assembly of aptamers and other probes on the electrode surface plays an important role in the nanoarchitectonics of optical drug biosensors. Different methods have been applied in various research works for the manufacturing of cocaine calorimetric and fluorescent biosensors. Xia et al. used colorimetry sensing with a single strand DNA (ssDNA) probe, unmodified gold nanoparticles, and a water-soluble conjugated polyelectrolyte with a positive charge to detect a wide variety of targets, such as DNA sequences, proteins, and small molecules including cocaine in minutes with no substantial apparatus or training expenses.[161] This highly versatile technique relies on ssDNA to prevent the aggregation of gold nanoparticles. The conjugated polyelectrolyte suppresses this capability, which is not observed with double-stranded or otherwise "folded" DNA constructs. They employed the anticocaine aptamer of Stojanovic[146,148] that was cut into two short single-stranded fragments. In the absence of cocaine, the addition of polyelectrolyte into the gold solution changes the color from red to blue due to the gold aggregation. In the presence of cocaine, the complex cocaine-aptamer structure weakly binds with the conjugated polyelectrolyte retaining its red color. Colorimetry-based tests applying this mechanism to recognize hybridization are sensitive and convenient, with simple detection of picomolar concentrations of target DNA by the naked eye. The sensor performs even in complex sample milieus, including blood serum.

In addition, smart molecules and functional materials also provide versatile frameworks for the development of optical drug biosensors. Structure-switching probes and aptamers improve the selectivity of the biosensor and potentially provide a multiplex platform for multi-drug recognition. Zheng et al. employed structure-switching aptamers (SSAs), SYBR Gold fluorescent dye, and exonuclease using a label-free sensing method to detect a wide variety of targets, including cocaine, in urine and serum.[162] SSAs when coupled with their targets fold into secondary constructs such as a quadruplex construct or a Y-shaped construct in the case of cocaine and become more resistant to nuclease digestion than unfolded SSAs. This phenomenon led to strong fluorescence in the presence of SYBR

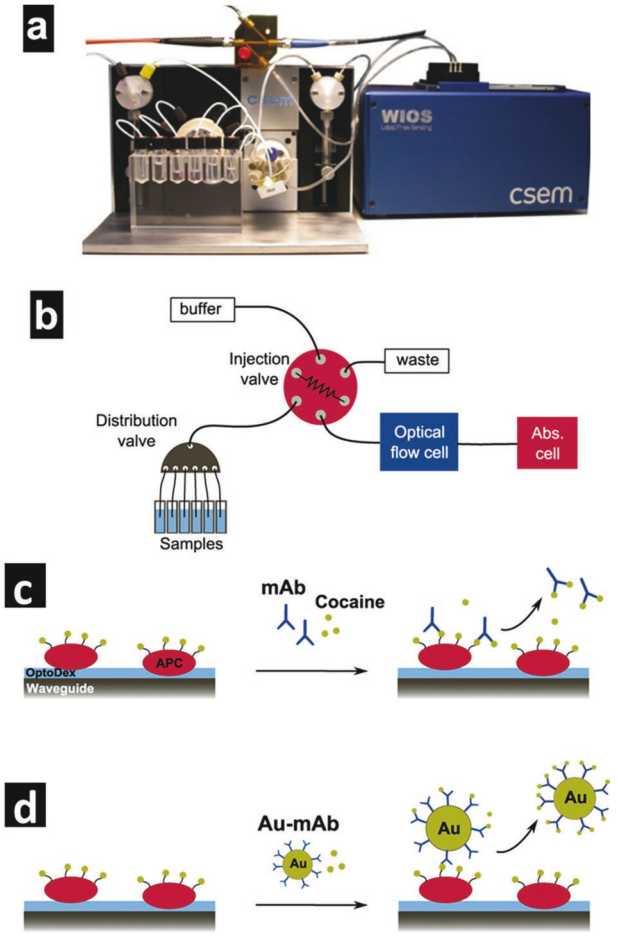

Figure 9. Biosensing mechanism a) setup. b) components. c) mAb and d) Au-mAb. Reproduced with permission.[160] Copyright 2012, Elsevier.

gold with the fluorescence intensity proportional to the concentration of cocaine. For direct use in cocaine detection, urine samples were passed through 0.22×10^{-6} M membranes. In nonoptimal settings, the test had an estimated cocaine LOD of 5×10^{-6} M (S/N = 3), which is competitive with other labeled fluorescent techniques. Compared to the effect of switching-structure probes in electrochemical biosensors, the observed improvement in the detection limit of this optical biosensor is negligible. This is mainly because the electron transfer process is enhanced in electrochemical biosensors which is not applicable in optical biosensors.

Another aspect of target-responsive probes implementation in the nanoarchitecture of optical drug biosensors is configuration alteration. In the presence of a target molecule, a configuration change in the aptamer sequences may be triggered and a combination of some complementary sequences may happen. This capability is very promising for the development of drug biosensors with high selectivity. Zhou et al. used minor groove binder-based energy transfer to develop a fluorescence optical aptasensor of cocaine.[97] The conformation of cocaine sensitive fluorescein isothiocyanate (FITC)-labeled aptamer changed from an incomplete ssDNA with a small hairpin to a double-stranded T-junction when the target was present. The DNA minor groove binder Hoechst 33342 prevented selective binding to the double-stranded T-junction, which brought the dye within the Förster radius of FITC, thereby triggering minor groove binder-based energy transfer, indicating the presence of cocaine. With a LOD of 0.2×10^{-6} M, the sensor was also applied on carboxy-functionalized polydimethylsiloxane (PDMS) surface with covalent immobilization of DNA aptamers. Surface-bound cocaine recognition plays a critical role in the development of microfluidic sensors.

The implementation of multifunctional materials and multimodal techniques is crucial for the development of multipurpose biosensors. Multiplex biosensing to recognize various abuse drugs or molecules and biomolecules will be accessible through further advancement in nanoarchitectonics of the appropriate probes and their assembly on a properly modified electrode. A report by Teller et al. indicates that the fabrication of a bifunctional sensor by haptenized acetylcholinesterase can be used for detecting cocaine and organophosphates[163] As shown in **Figure 11**, their designed dual piezoelectric/amperometric sensor aims to detect two unconnected analytes in one assay using propidium to anchor acetylcholinesterases (AChE) to the surface. In addition to allowing the investigation of the interplay between AChE and the modified surface, this mass-sensitive sensor also enables detection of in situ suppression of the surface-coupled AChE. The cocaine derivative benzoylecgonine (BZE) was linked to carboxylate groups of the AChE through a 10 Å length hydrophilic linker 1,8-diamino-3,4-dioxaoctane-following activation of EDC/NHS. The modified AChE (BZE-AChE) contains an extra recognition agent in addition to the inhibitory coupling site. It is possible to monitor the coupling

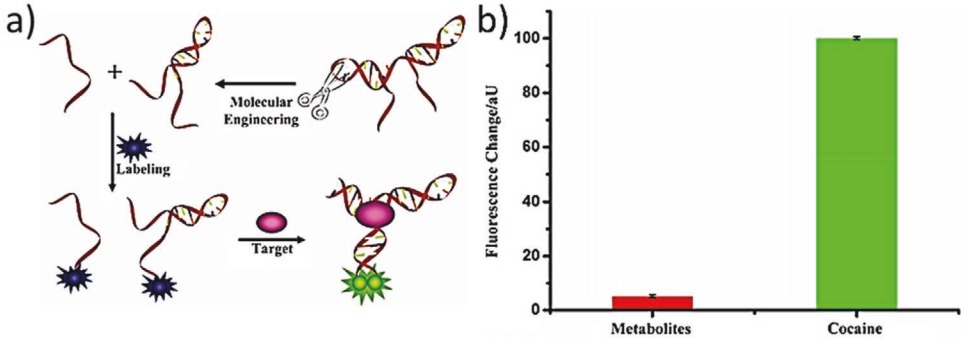

Figure 10. a) Working principle of light-switching excimer sensor based on target induced complementary aptamer fragments (CAF). b) Responses of CAF sensor to cocaine and its metabolites. Reproduced with permission.[107] Copyright 2010, Elsevier.

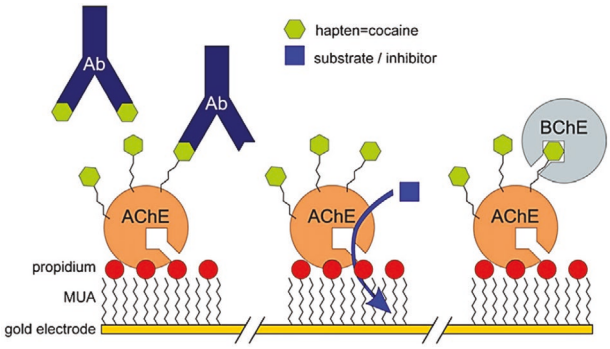

Figure 11. The sensing mechanism of BZE-AChE on a propidium-modified sensor. From left to right: interaction with the anti-BZE-antibody, substrate conversion or inhibition of the immobilized enzyme, interaction with huBChE. Reproduced with permission.[163] Copyright 2008, Elsevier.

of an anti-BZE-antibody to the BZE-AChE when the BZE-AChE deposits on the sensor surface. Two analytes (cocaine and organophosphate) are detected simultaneously by measuring antibody coupling and reduction of enzymatic action, respectively. Additionally, other cocaine-binding enzymes, such as butyrylcholinesterase, were capable of binding to the modified BZE-AChE. The competitive immunoassay made it possible to detect cocaine in a dynamic range between 10^{-9} and 10^{-7} M.

As shown schematically in **Figure 12**, Voyvodic et al.[164] demonstrated a different arrangement of plug-and-play metabolic transducers to expand the chemical recognition space of cell-free biosensors. Their biosensor includes the transcription factor BenR, which is actuated by benzoic acid, and two metabolic modules HipO and CocE, which convert hippuric acid and cocaine into benzoic acid respectively. Every element is separately cloned into a cell-free vector, making it possible to titrate DNA concentrations over three orders of magnitude to optimize sensor functionality. These researchers showed that the sensors could operate in complex solutions, identifying benzoic acid in commercial beverages and hippuric acid and cocaine in human urine (Figure 12).

A cocaine sensor with high sensitivity, reliant on a nanochannel alone, with attached DNA aptamers, was designed by Wang et al.[165] Target cocaine concentrations and output ionic current are linearly correlated at concentrations of 1×10^{-9} M–10×10^{-6} M. This cocaine sensor has a LOD down to 1×10^{-9} M. A schematic of this cocaine biosensor is depicted in **Figure 13**.

Alternatively, Zhang et al. reported a method for an aptamer-intermediate microfluidic beads-based sensor to detect and quantify multiple analytes using multi-enzyme-linked nanoparticle amplification and quantum dot labels.[115] Adenosine and cocaine were chosen as the model analytes for validating the test scheme based on strand dislocation stimulated by the formation of a target-aptamer complex. Microbeads, functionalized with the aptamers and modified electron-replete proteins, were arranged inside a microfluidic channel and coupled with HRP to capture DNA probe derivative AuNPs through hybridization. The findings demonstrated that the microfluidic-based technique was a fast and effective system for testing aptamer-based targets (adenosine 0.1×10^{-12} M and cocaine 0.5×10^{-12} M), which required only minimal amounts (microliter) of reagent.

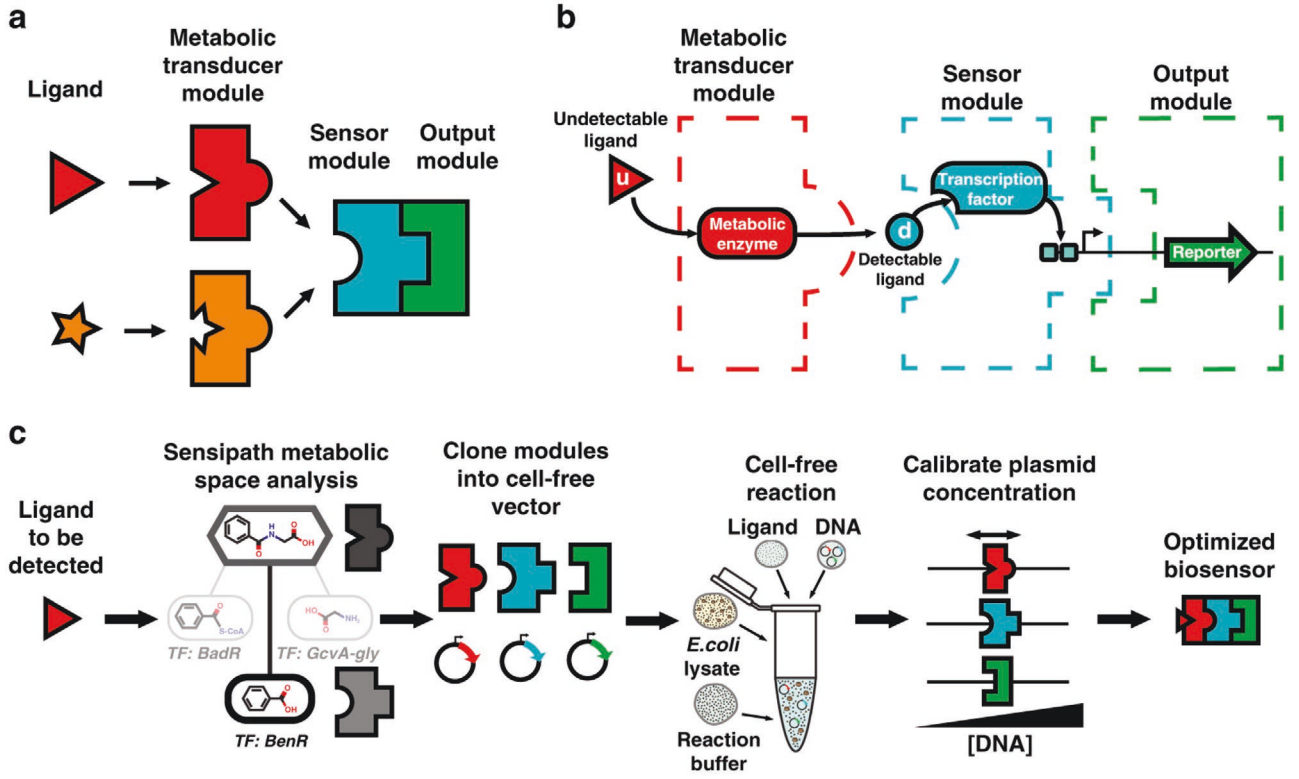

Figure 12. Schematic representation of cell-free biosensors: a) Cell-free biosensors modules. b) The undetectable ligand is converted by an enzyme into a detectable one. c) The biosensor operates through a retrosynthetic mechanism. Reproduced with permission.[164] Copyright 2019, Nature.

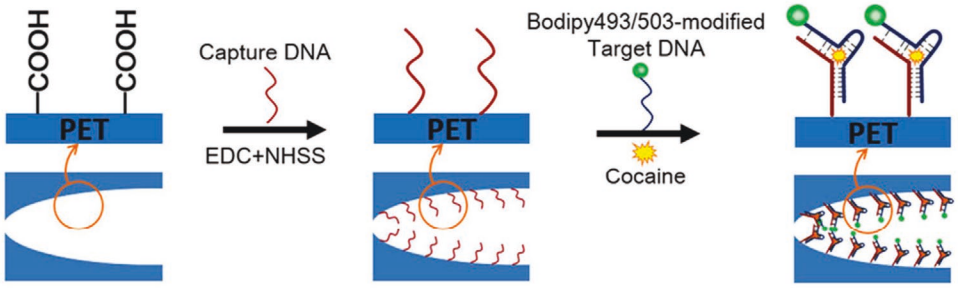

Figure 13. Schema of an aptamer-based cocaine detector using a single nanochannel. ssDNA was used to functionalize the nanochannel and fold into dsDNA through cocaine binding, changing electron transfer, and reducing the current as of the main signal. Cocaine could be directly measured by the current recording. The oligonucleotide sequence (5' to 3') of Capture DNA is 5'-NH_2-$(CH_2)_3$GGGAGTCAAGAACGAA-3', and the oligonucleotide sequence (5' to 3') of Target DNA is 5'-Bodipy493/503-TTCGTTCTTCAATGAAGTGGGACGACA-3'. Reproduced with permission.[165] Copyright 2018, American Chemical Society.

All types of reported cocaine biosensors potentially could be progressed and commercialized but electrochemical cocaine biosensors are probably the most promising. Effective use of structure-switching and smart functional materials in nanoarchitecting of cocaine biosensors will provide a platform for not only single molecular recognition but also multiplexed biological detection.

3.2. Codeine Sensing

Codeine is the o-methylated form of morphine and is categorized as an opioid drug. Despite the low affinity of codeine to μ-opiate receptors, its active opioid-based metabolite in the body is morphine. Although the major fraction of codeine undergoes glucuronidation to form codeine-6-glucuronide, accidental and intentional overdosing can occur.

AChE coated on a screen-printed carbon electrode (SPCE) is a promising approach for biosensing codeine.[166] Codeine inhibits AChE cross-linked on SPCE from converting acetylthiocholine (ATI) to thiocholine, which undergoes dimerization in the presence of an oxidized form of tetrathiafulvalene (TTF). This mediates the chronoamperometric process, an efficient electrochemical technique in which the generated current from faradaic processes is monitored as a function of time (**Figure 14**).[166] In this method, the electrical potential of +250 mV versus screen-printed Ag/AgCl electrode and supporting electrolyte, pH 7 is applied with a detection limit of 20×10^{-6} M.[166] Cytochrome P450 2D6 (CYP2D6), the specific enzyme that converts codeine to morphine has been utilized for electrochemical biosensing of codeine through the covalent coating on SPCE[167] (**Figure 15**). A potential of +250 mV and pH of 7 with an Ag/AgCl screen-printed electrode was employed for the detection of codeine in the concentration range of 20×10^{-6}–200×10^{-6} M.[167]

Benzylisoquinoline alkaloids (BIA), are plant-specialized metabolites and include opioid compounds such as codeine and morphine which are found in some natural sources of opioids such as the opium poppy (*Papaver somniferum*). Detection of BIA can be a useful method to judge if the source of an opioid is natural. However, there are few reported techniques for the detection of BIAs.[168] Electrochemical oxidation of morphine and codeine merged on a pencil graphite electrode (PGE), modified with double-stranded DNA (dsDNA) and multiwall carbon nanotubes (MWCNT) has been used to measure codeine.[169] In this work, poly(diallyldimethylammonium chloride) (PDDA) was used as a dispersant for MWCNTs. The amino and phenolic groups in morphine and codeine are oxidized under DPV at a PGE. Morphine and codeine electrochemical signals moved to more positive and negative potentials respectively after the addition of DNA to the system. As the DNA concentration increased two anodic peaks of codeine were observed. A difference in the peaks of morphine and codeine was seen. The intercalation mechanism was identified for morphine and an electrostatic

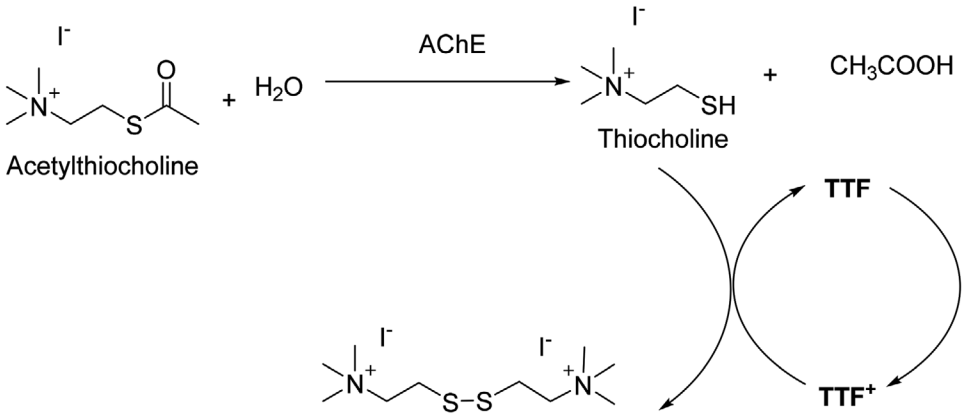

Figure 14. The mechanism of codeine biosensing in the presence of AChE-coated SPCE. Adapted with permission.[166] Copyright 2013, Elsevier.

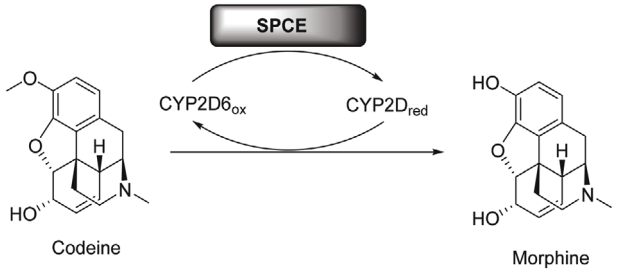

Figure 15. Representation of codeine biotransformation to morphine by cytochrome P450 2D6 enzyme catalyst. Adapted with permission.[167] Copyright 2014, Elsevier.

mechanism for codeine. The linear dynamic range for morphine was between 0.05 and 42 μg mL^{-1} and for codeine was between 0.05 and 40 μg mL^{-1} (ignoring the first five minutes accumulation period, when 0.043 and 0.041 μg mL^{-1} was the detection time for morphine and codeine, respectively). In the case of codeine, three different groups are undergoing oxidation at a certain pH. Electrochemical measurement at a pH in the range of 2–8 results in two anodic peaks which are attributed to oxidation of tertiary amine and the 6-hydroxy groups of codeine. At pH of 8, one additional anodic peak is observed which is originated from the oxidation of the 3-methoxy group, and at a higher pH, further oxidation of the secondary amine group from the oxidation of the tertiary amine group. Moreover, the shift and number of peaks depended on the amount of dsDNA. In this study, morphine and codeine were detected in pharmaceutical formulations, urine and blood serum samples.[169]

In 1995, Lowe and co-workers used the first enzymatic method for the detection of heroin, morphine, and their metabolites, e.g., morphine-3-glucuronide. They used two enzymes, morphine dehydrogenase (MDH) and acetylmorphine carboxylesterase (heroin esterase), in an amperometric assay with a detection limit of 23.7×10^{-6} M (for morphine) using phenazine methosulphate as a mediator.[170,171] The use of a mediator is necessary since the elector-oxidation of compounds like codeine requires a high potential. Therefore, they use mediators such as phenazine methosulphate or TTF.

SELEX method has been utilized to produce DNA aptamers against codeine (**Figure 16**).[17] The HL7-14 aptamer which is a 37-mer sequence exhibited a stronger selectivity toward codeine than morphine or other molecules with a dissociation constant (K_d) of 0.91×10^{-6} M. The aptamer clone in this method is composed of a 39 mer selected from DNA molecules and a 45 mer random region. This aptamer is cut into two G-T wobble base pairs in a CTGTTT 3' end cut with HL7-1. The high specificity of HL7-14 to codeine prevents it from binding small compounds. $[Fe(CN)_6]^{3-/4-}$ was used as an electroactive redox probe to scrutinize label-free electrochemical codeine aptasensor, with aptamers immobilized on the substrate of Au-mesoporous silica nanoparticles (Au-MSN). A pH of 7.4, a high concentration of Na^+ (500×10^{-3} M), and K^+ concentration in the range of $0–10 \times 10^{-3}$ M resulted in the highest affinity of the aptamer to codeine. The detection limit was 3×10^{-12} M and the correlation coefficient 0.9979, over a linear range between 10×10^{-12} M to 100×10^{-9} M.[17]

In a study by Niu et al.,[172] the surface of SPCEs was functionalized with gold nanoparticles, absorbed with the help of polyamidoamine dendrimers (PAMAM). Immobilization of the codeine aptamer was performed over a glutaraldehyde (GA)/chitosan (CHIT)/PAMAM adjusted electrode (**Figure 17**). The authors claimed that PAMAM facilitated Au immobilization on the electrode resulting in a high number of codeine aptamers available for codeine detection. Moreover, the insulating properties of PAMAM also inhibit the electrochemical probe, in this case, $K_3Fe(CN)_6/K_4Fe(CN)_6$ from reaching the SPCE surface, hence the impedance of the electrode is relatively high. However, the effect of the amount of PAMAM was not reported. Codeine detection is based on the prevention of electron transfer of the electrochemical probe $K_3Fe(CN)_6/K_4Fe(CN)_6$ by binding codeine to the aptamer. The detection limit was 3×10^{-13} in the range of 1×10^{-12}–1×10^{-7} M. With fast detection, a broad detection range, and a lower detection limit, this sensor could be used for codeine biosensing in aqueous solutions including blood serum. They also found that 80 minutes was the optimal incubation time to obtain the highest sensing result.[172]

Saberian et al.[173] developed another aptamer-based biosensor to identify codeine in nanomolar concentrations, using an electrochemical method with ferrocene carboxylic redox molecule. The formation of the codeine-aptamer complex reduces the spatial distance between the redox molecule and the electrode surface, increasing charge transfer, and raising the redox current. Zhou et al.[174] showed amperometric detection of codeine and its metabolite, morphine after capillary region electrophoretic separation. Using a carbon disk electrode, a response of 0.90 V (vs Ag/AgCl) was achieved. Morphine and codeine detection limits were 6.8×10^{-8} and 1.6×10^{-7} M, respectively, with a linear range of 1.9×10^{-7}–1.5×10^{-5} M for morphine (0.9999 correlation coefficient) and 3.1×10^{-7}–2.5×10^{-5} M (0.9996 correlation coefficient) for codeine under optimal conditions of detection and separation (12 kV voltage, 0.06 M phosphate

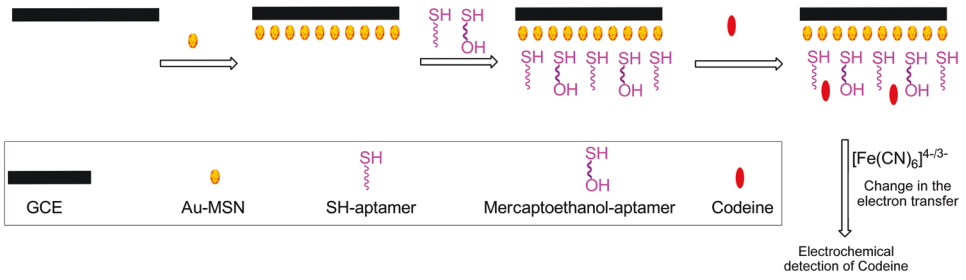

Figure 16. The schematic representation of electrochemical codeine aptasensor. Adapted with permission.[17] Copyright 2013, Elsevier.

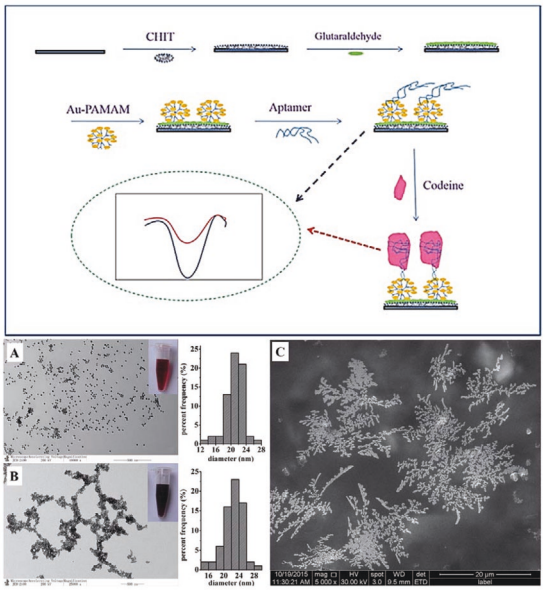

Figure 17. Schematic representation of GA/ CHIT/PAMAM electrode and immobilization of codeine aptamer. Transmission electron microscopy (TEM) image: A) Au NPs and B) Au NP/PAMAM. C) Scanning electron microscopy (SEM) images of Au NP/PAMAM/GA/CHIT/SPCE. Adapted with permission.[172] Copyright 2016, Royal Society of Chemistry.

buffer solution and pH of 8.4). The technique was applied to filtered samples of morphine and codeine in human urine, without any interference despite the complex composition of the sample, making it a promising approach for pharmacology and pharmacokinetic studies as well as for drug abuse detection, supervising clinical intoxication episodes, forensic and therapeutic applications.[174]

In summary, the most effective biosensor strategies for the detection of codeine are based on electrochemical techniques. The developed nanoarchitectonics for fabrication of appropriate electrodes and easing electron transfer provides a versatile and promising platform for codeine sensing devices.

3.3. Heroin Sensing

Heroin or 3,6-diacetylmorphine, diamorphine is a morphine derivative that is highly addictive. Recently, the U.S. has witnessed a sharp increase in heroin usage as well as heroin overdoses. Drug abusers or people showing signs of dependence on prescription opioids are 40 times more likely to abuse or become reliant on heroin in comparison with individuals that did not consume opioids for non-medical purposes.[175] A sharp increase in the percentage of individuals with heroin use disorder within 2010–2014 was observed in the 18–25 age group.[176] Likewise, national death data revealed high heroin overdose rates among younger age groups.[177] Heroin is regularly mixed with illicitly manufactured fentanyl (IMF), and deaths relating to synthetic opioids, such as fentanyl, are high in younger age groups.[177,178]

A system for the rapid recognition of narcotics, e.g., heroin, in vapor and dust medium was explored where a microfluidic vapor-to-liquid interface was paired to numerous downstream QCM sensors. A new micromachined interface, which is capable of robust sheet liquid flow was investigated to facilitate droplet-to-liquid transfer and airborne sample-to-liquid adsorption by Frisk et al.[138] 100 ng of heroin and 50 ng of cocaine were used, producing 50 Hz and 15 Hz frequencies, respectively. The reported QCM sensing approach was very fast with a short detection time. **Figure 18** illustrates the main components of the developed system and schematics of flow measurement.

Two-step conversion of heroin to morphine was carried out by Lowe et al. using two bacterial enzymes, heroin esterase, and morphine dehydrogenase. Heroin esterase converts heroin to morphine by hydrolyzing acetyl ester groups of heroin. Meanwhile, morphine dehydrogenase with $NADP^+$ dependency acts as an oxidizing agent that oxidizes morphine to morphinone. (see **Figure 19**).[179] The oxidation of morphine to morphinone by morphine dehydrogenase is linked to a bacterial luciferase so the reaction generates light as a detection signal. In urine, heroin in a solid particulate drug form was detected. In this bioluminescent assay, the sensitivity for morphine and heroin was 2.0 and 89 ng mL^{-1} respectively. However, the immobilized forms of the enzymes exhibited higher sensitivity for heroin (101 ng, equal to 250 pmol), corresponding to 1–2 particles of illegal heroin.[179] **Figure 20** shows the mechanism of the bioluminescent enzyme assay for heroin and its metabolites using bacterial Luciferase. A similar strategy was used by Rathbone et al.[180] The main heroin-morphine conversion reactions used in their enzymatic assay are shown in **Figure 21**.

Recently, Salimi et al. used glassy carbon electrode (GCE), with graphene nanosheets (GNSs) for concurrent determination of well-known opiate drugs, i.e., heroin, noscapine, and morphine, based on electrochemical oxidation.[181] Electrocatalytic activity versus oxidation of these components was achieved in a broad range of pH values and decreased overpotentials. With the voltammetry method, the oxidation of those analytes depends on the pH value and 8 is the optimal pH to differentiate heroin, noscapine, and morphine. At this pH, heroin is hydrolyzed to monoacetyl morphine, which involves charge transfer between heroin and the electrode. The DPV calibration curves showed detection limits of 0.5×10^{-6}, 0.2×10^{-6}, and 0.4×10^{-6} M for heroin, noscapine, and morphine, the sensitivity of 217, 500, 275 nA μM^{-1} cm^{-2} and a linear dynamic range of 100×10^{-6}, 40×10^{-6}, 65×10^{-6} M, respectively. This sensor does not require a particular reagent or electron-delivery mediator, pretreatment, or separation phases, allowing for concurrent or separate detection of these chemicals with a modified electrode.[181]

Heroin has been also detected by an ECL sensor which contains a molecularly imprinted polymer deposited on an MWCNT-Nafion composite modified electrode. Before composite modification, the GCE electrode was also modified by Ru_3^{2+}. This technique utilizes the molecular memory of the electrode to heroin after template removal. Shang et al.[182] reported a heroin sensor which had a detection limit of 4.0×10^{-15} M (S/N = 3) with a linear response range of 1.0×10^{-14}–1.0×10^{-10} M with an incubation time of 5 min in 0.1 M PBS and a scan velocity of 100 mV s^{-1}. Their sensor was

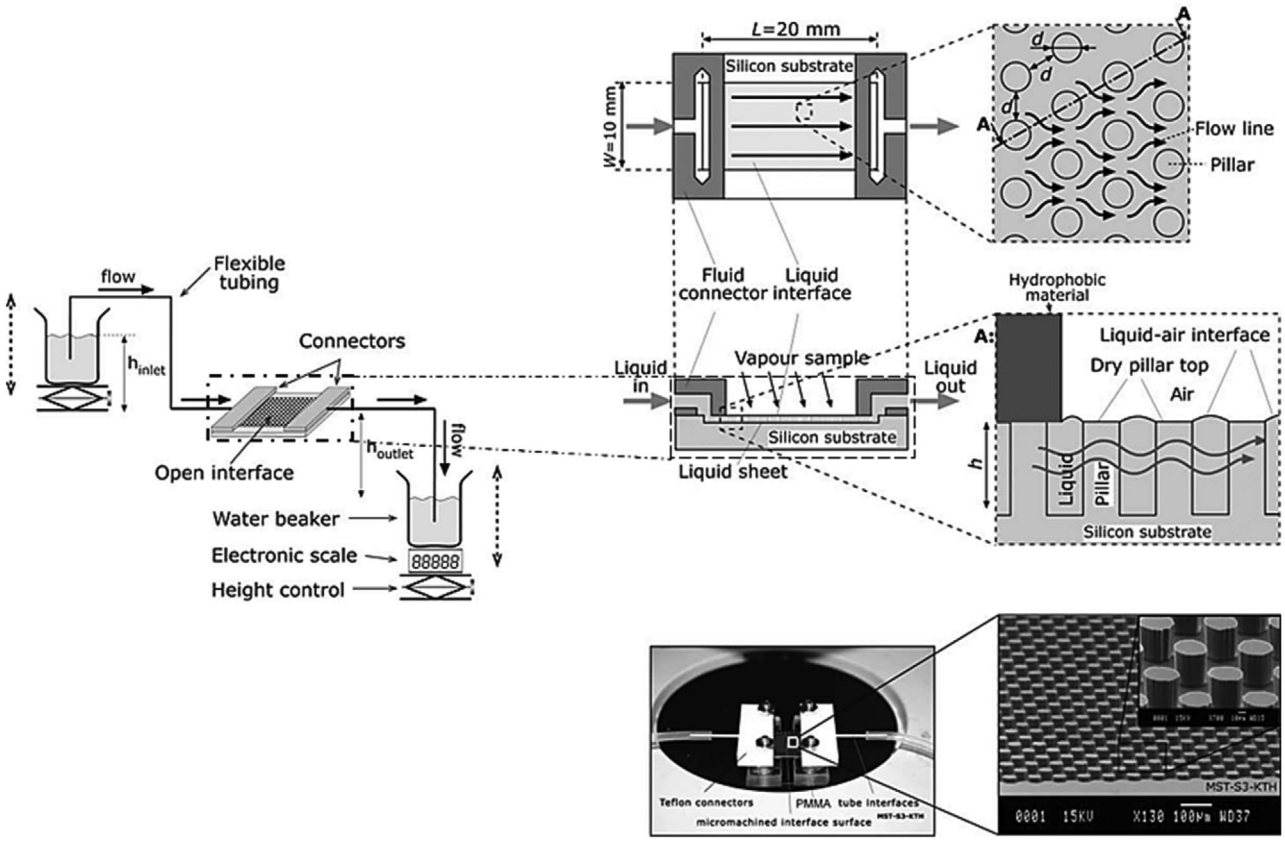

Figure 18. Schematics of flow measurement. SEM micrograph showing the pillared structure of the silicon QCM surface. Reproduced with permission.[138] Copyright 2006, Royal Society of Chemistry.

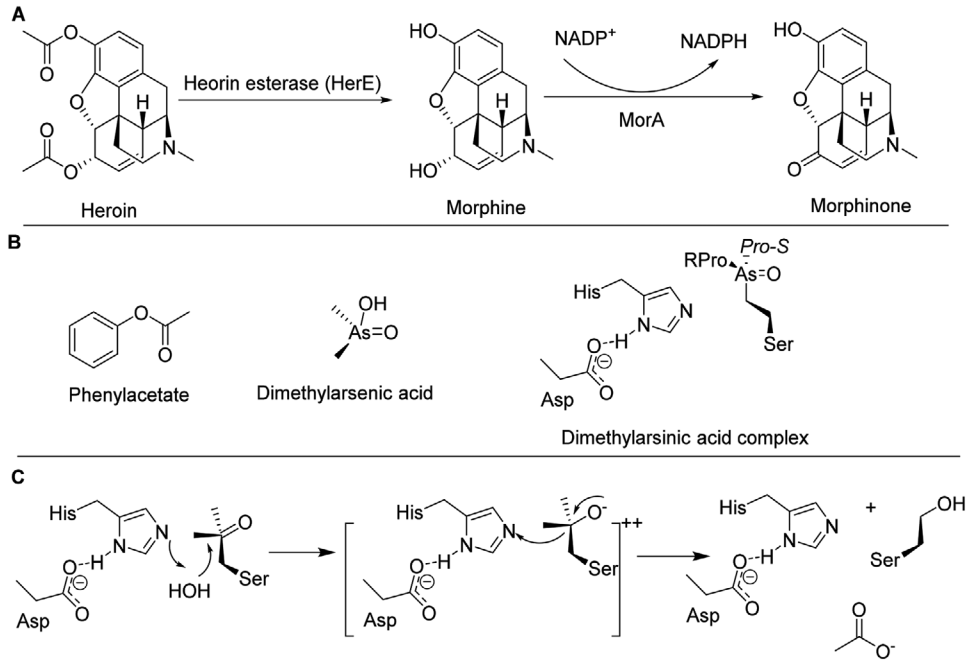

Figure 19. Reactions involved in linked-enzyme assay for both heroin and its metabolites.[179]

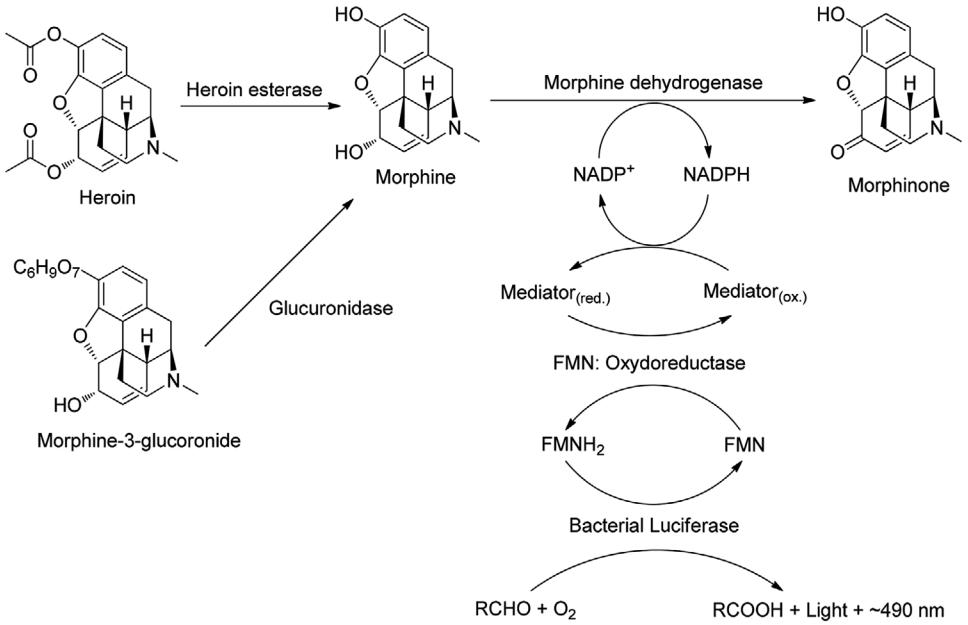

Figure 20. Schematic representation of the bioluminescent enzyme assay for heroin and its metabolites through bacterial Luciferase.[179]

designed on a remodified molecularly imprinted polymer film onto $Ru(bpy)_3^{2+}$ modified glassy carbon electrode.

The other technique that has been used for the detection of heroin is a field-effect, liquid-gated transistor based on CNT which was reported by Mhaisalkar et al.[183] In this method, the CNTs are functionalized with a receptor–ligand, which produces electrostatic perturbation, which is increased by charged Au nanoparticles. The immunoassay protocol was able to detect monoacetylmorphine (MAM) down to 15 pg mL^{-1}. Morphine-derived compounds can be detected using this competitive assay and a liquid-gated field-effect transistor based on p-type CNT. CNT channel conductance depends on the doping of the CNT network. In this approach, monoacetylmorphine-bovine serum albumin (MAM-BSA) was the target for MOR-1-antibody (Mor-Ab) (**Figure 22**). A rise in drain current was observed for Mor-Ab with negatively charged Au NPs.[183]

ECL and QCM techniques are an appropriate class of sensors for reliable and precise sensing of heroin, due to reported detection limits and linear response range. Nanoarchitectonics for the fabrication of QCM and ECL sensors has been implemented for the effective immobilization of receptors and decorating of nanoparticles.

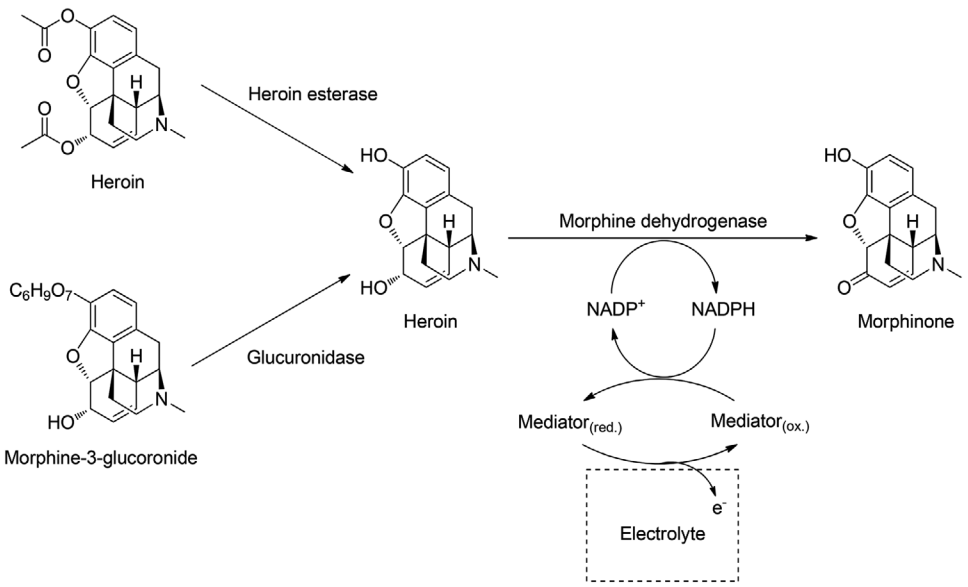

Figure 21. Reactions associated with the enzymatic conversion of heroin and morphine applied in biosensing approaches.[180]

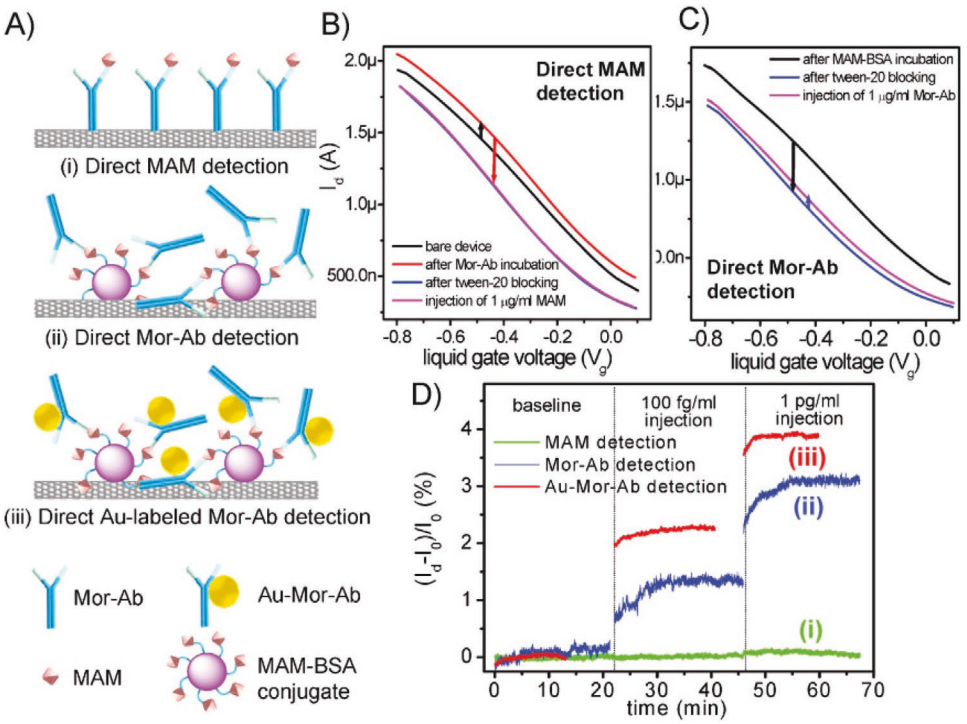

Figure 22. A) Schema of direct assay biosensing approaches: i) MAM, ii) Mor-Ab, and iii) Au-labeled Mor-Ab (Au-Mor-Ab) as the target analyte. B,C) Comparison of drain current (Ids) versus gate-source voltage (V_g) plots of direct assay schemes: i,ii) Injection of 1 μg mL^{-1} MAM into the liquid-gated field-effect transistor (LGFET) yields no change in the current. D) Normalized plots for kinetic measurements of direct assay approaches. Reproduced with permission.[183] Copyright 2010, Wiley-VCH.

3.4. Morphine Sensing

Morphine is an opioid analgesic that is commonly used for pain management however it has dangerous side effects including addiction, analgesic tolerance, gastrointestinal symptoms, and immunosuppression.[184] Several techniques including optic and electrochemical methods have been used for morphine detection. For instance, a CNT-liquid gate transistor was used to detect the opiate drug in a real-time and label-free technique in a study by Tey et al.[185] This device was fabricated using a two-step stamping and lamination process, enabling large-scale processing at room temperature. They used the indirect Mor-Ab for detection to reduce the charge screening effect by the electrolyte ions and maximize electronic signal (depicted in **Figure 23**). In their approach, MAM-BSA was bound covalently with carboxylated-CNTs. The addition of Mor-Ab that is negatively charged induces an increase in hole concentration in p-type CNT modulating electrical current. The detection of Mor-Ab on this system resulted in a LOD of 130 fg mL^{-1} with a detection range of 10 fg mL^{-1}–100 ng mL^{-1}. When Mor-Ab was modified with AuNPs to increase the signal amplification the LOD was reduced to 1 fg mL^{-1}.[185]

Exfoliation of layered materials, e.g., graphene-based materials, is a useful technique to overcome the inactivation of the interlayer space through self-assembly phenomenon.[186–189] An amperometric morphine sensor has been developed using an exfoliated graphene oxide (EGO) modified screen-printed electrode. EGO is believed to provide abundant active sites due to the presence of numerous functional groups on its surface. These groups support the oxidation of morphine involving charge transfer that is delivered as a current signal. The sensors display a detection limit of 2.5 ppb and sensitivity of 2.61 nA ppb^{-1} using electrocatalytic processes in a study by Maccaferri et al.[190] Interestingly, this work also measured morphine in urine samples that normally contain uric acid. Although the uric acid gives a high signal at a different potential, the morphine signal was very low. To solve this problem, they proposed a five to one dilution.

Antigen-dependent elimination of fluorescence quenching phenomenon was used in a reagent-free fluorescent biosensor in a study by Ueda et al.[191] As shown in **Figure 24** a single-chain fragment variable (scFv) antibody was fluorolabeled

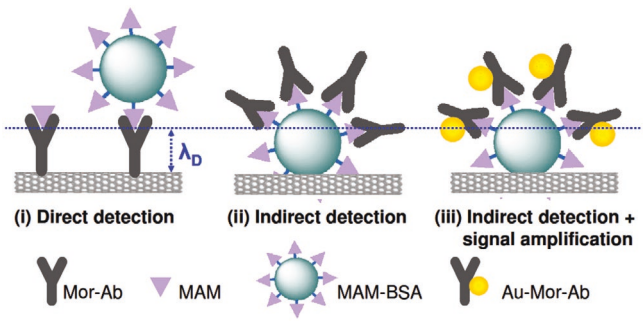

Figure 23. Indirect and direct detection methods for morphine. Reproduced with permission.[185] Copyright 2010, NSTI-Nanotech.

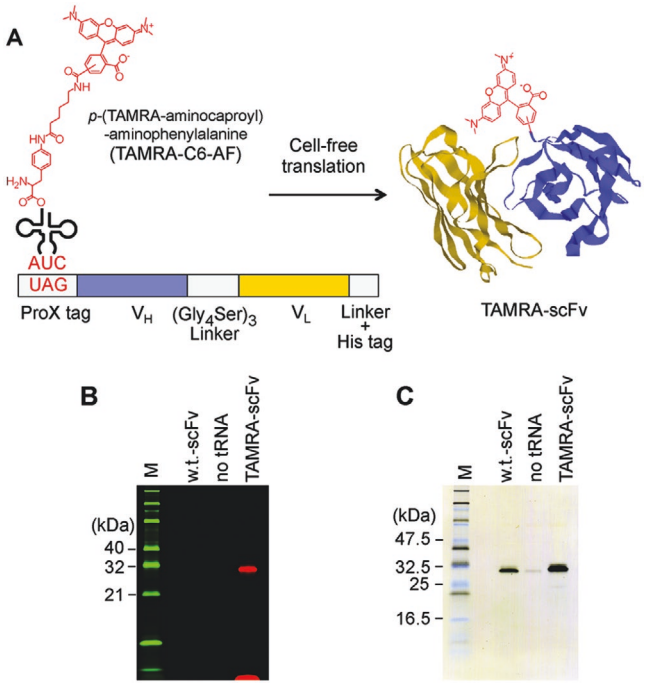

Figure 24. A) scFv production with TAMRA labeling at the *N*-terminus. In a translational and cell-free system, UAG reaction to the combination of scFV and TAMRA-C6-AF is demonstrated. B) SDS-PAGE fluorescence image. Green colored TAMRA fluorescence line was observed with 580 nm emission and 532 nm excitation while a red-colored line was observed with 520 nm emission and 488 nm excitation. C) Anti-His-tag was used to analyze the western blot in a figure which is Reproduced with permission.[191] Copyright 2011, American Chemical Society.

at the *N*-terminal end, with the help of cell-free translation-mediated position-specific protein labeling. In the mutagenesis process, carboxytetramethylrhodamine (TAMRA)-labeled anti-osteocalcin scFv was used. The binding of antigen disrupted the quenching effect due to the proximity of tryptophan residues to the linker-tagged fluorophore. Proteins, peptides, and haptens of drugs related to morphine were detected with TAMRA-scFv in human plasma.

Electrochemical detection of morphine in urine using screen-printed carbon electrodes and electromembrane extraction (EME) was achieved by Fakhri et al.[192] Their EME strategy utilizes charge separation between the donor solution containing morphine and the acceptor solution inside a supported liquid membrane (SLM). At a certain applied potential, the positively charged morphine migrates to the negative electrode containing SLM and platinum wire. After extraction, the organic solution containing separated morphine was collected and dropped on SPCE. The extraction process utilized different solvents of the donor solution (water) and the acceptor solution (organic), preventing negatively or neutral charged molecules and molecules with log P > one from being extracted in SLM. This morphine sensor achieved high selectivity. The electrochemical measurement displays a linear range between 0.005 and 2.0 µg mL^{-1} with a 0.005 µg mL^{-1} limit of detection.[192] An image of the produced strip sensor and associated components are shown in **Figure 25**. Moreover, this technique was also

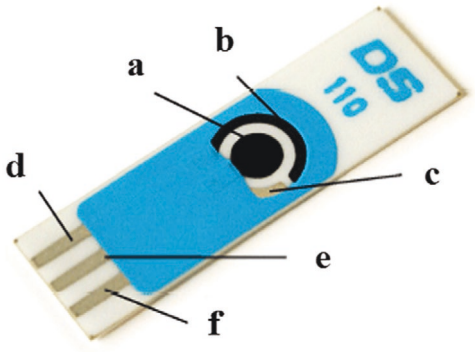

Figure 25. Image of the strip sensor: a) working electrode, b) counter electrode, c) reference electrode, d) counter electrode connection, e) working electrode connection, and f) reference electrode connection. Reproduced with permission.[192] Copyright 2014, Elsevier.

applied to detect morphine in urine samples with recoveries in the range of 71%–76%.

A mouse immune phage library was utilized in a study by Sugimura et al.[193] where morphine-conjugated BSA was applied to detach a scFv clone, M86, with affinity to morphine-conjugated thyroglobulin (morphine-C-Tg). Using SPR, a morphine-C-Tg-coupled CM5 sensor was fabricated for morphine detection with a K_d value of 1.26×10^{-8} M. By introducing numerous doses of free morphine and relevant compounds, a competing enzyme-linked immunosorbent assay (ELISA) with M86 and morphine-C-Tg was carried out to determine the coupling of free morphine and relevant compounds with M86. The IC_{50} for opium, morphine, codeine, and heroin was 257 ng mL^{-1}, 36.4×10^{-9}, 7.3×10^{-9}, and 7.4×10^{-9} M, accordingly. **Figure 26** illustrates the two main conjugation processes of narcotics with protein (Tg or BSA) which facilitate their recognition, and **Figure 27** shows the different simulated conformations of the M86 scFV and drugs combination.[193]

For detecting morphine-3-glucuronide (M3G), the major metabolite of heroin and morphine, in PBS and urine, Dillon et al.[25] developed two sensor systems: competitive ELISA immunoassays and BIAcore-based inhibition immunoassays. Both techniques used two polyclonal anti-M3 G rabbit antibodies. The competitive ELISA immunoassay detected a low concentration of M3G in PBS or urine. The reported detection ranges for M3G are 244–250 pg mL^{-1} and 61–31.250 pg mL^{-1} for Ab_1 and Ab_2, respectively. For the BIAcore inhibition assays, the reported detection ranges are 762–24.4 pg mL^{-1} and 976–31.25 pg mL^{-1} for Ab_1 and Ab_2, respectively.

Utilizing genetic material extracted from the spleen cells of mice immunized with morphine-3-glucuronide-bovine serum albumin (M3G-BSA) conjugate, Dillon et al.[194] recombined an scFv antibody with M3G. There is an inverse relationship between the antibody coupling to the surface of the chip and the amount of free drug in the solution. Optimizing the recovery conditions for antibody binding to the surface resulted in a binding-recovery capacity of at least 30 cycles. The inhibition assay ranges for M3G varied between 3 and 195 ng mL^{-1} and 3 and 97 ng mL^{-1} in PBS and urine, correspondingly.[195]

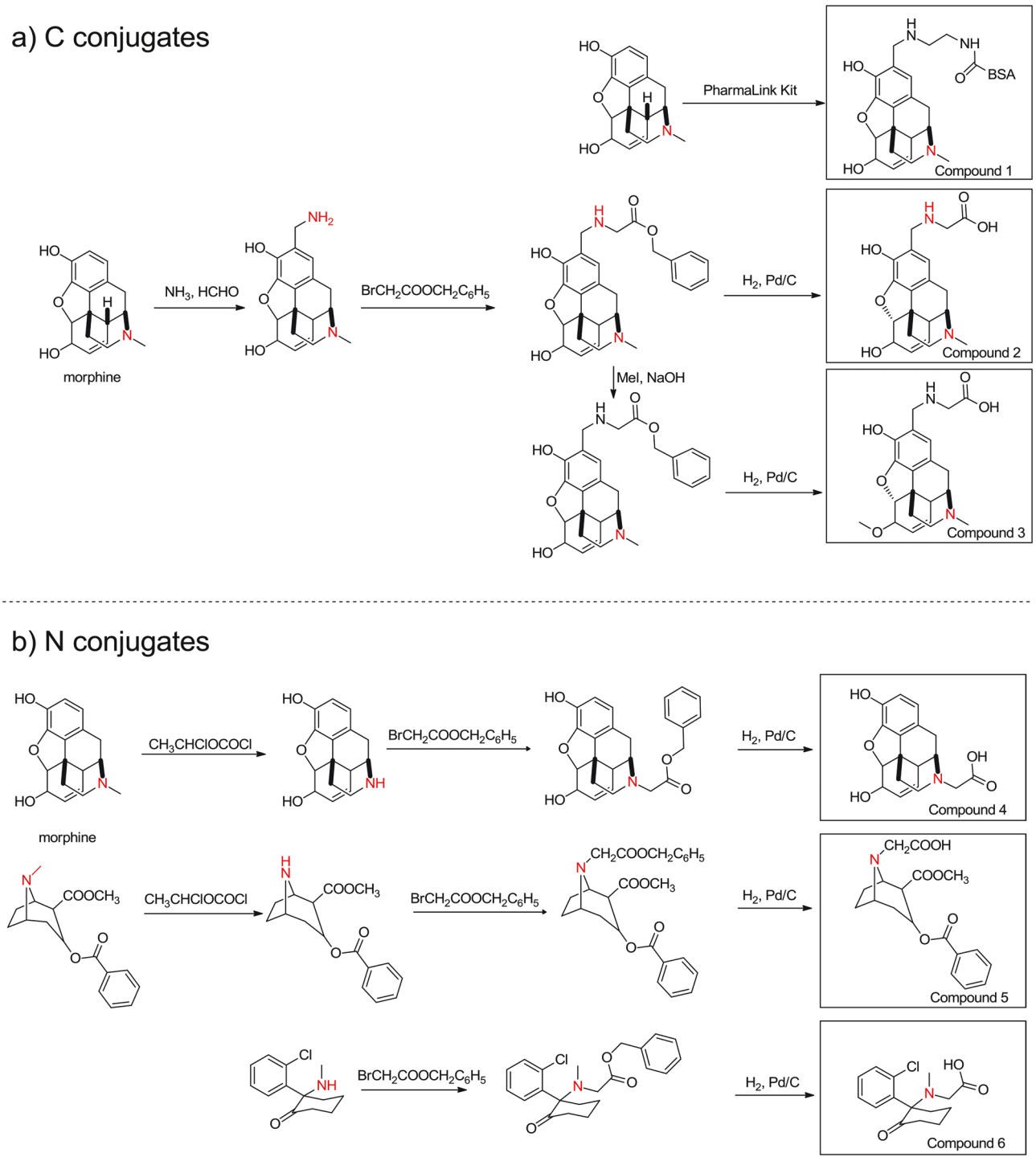

Figure 26. Conjugation of narcotics with protein (Tg or BSA). a) C conjugate derivatives. b) N conjugate derivatives. Adapted with permission.[193] Copyright 2013, MDPI.

Modification of MWCNTs with ionic liquids can have a drastic impact on the performance of the electrode. Modification of MWCNTs-carbon paste electrode with an ionic liquid, n-hexyl-3-methylimidazolium hexafluorophosphate, was used by Ensafi's group to measure morphine.[196] Cyclic voltammetry, chronoamperometry, and EIS were used to measure morphine at the modified electrode. The highest irreversible oxidation was achieved with a cyclic voltammogram at 0.48 V (vs $Ag/AgCl_{sat}$). DPV with optimized conditions resulted in an oxidation peak current of morphine, with two linear dynamic ranges (in 0.6–600 $\times 10^{-6}$ M) and a detection limit of 0.02 $\times 10^{-6}$ M in human urine and injection solution.[196]

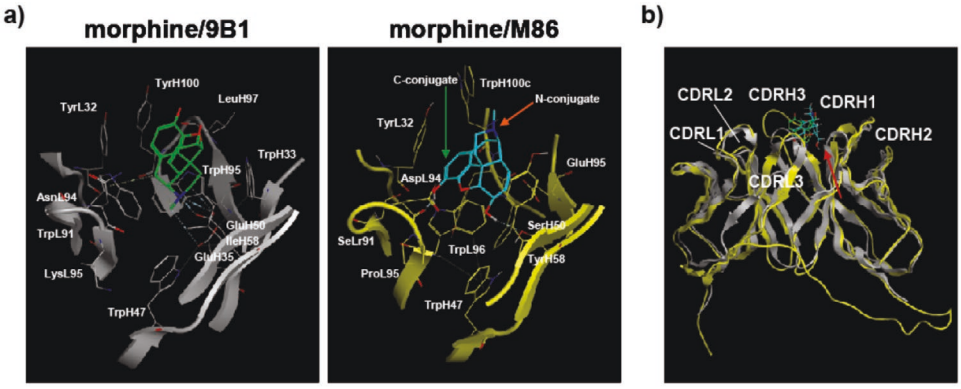

Figure 27. Conformations of M86 scFV. a) M86 and 9B1 ligand interaction surface—side view. b) Superposition of 9B1 and M86. The view direction is shown by the red arrow. Reproduced with permission.[193] Copyright 2013, MDPI.

Immunosensing chips for detection is another important advance in biosensing morphine. Yifeng et al.[197] produced an immunosensing chip for the detection of morphine with a QCM modified with 3-mercaptopropionic acid, activated by 1-ethyl-3-(3-dimethylaminoprephyl) carbodiimide and *N*-hydroxysulfosuccinimide to immobilize the MOR-Ab. The specific affinity between antibody and antigen allowed label-free detection of morphine, with a detection limit of 0.11 pg mL^{-1} and the linear range from 2 to 50 pg mL^{-1} in spiked human urine.[197] Kriz and Mosbach[198] introduced a morphine-sensitive device based on a molecularly imprinted polymer. The peak current (by oxidation) was 4 nA corresponding to a morphine concentration of 0.5 μg mL^{-1}. The method is a two-step process. In the first step, morphine binds to the molecularly imprinted polymer. In the second step, an excess electro-inactive competitor (codeine) was introduced to compete with bound morphine. An amperometric method measures the released amount of morphine.[198]

A label-free integrative pharmacology on-target (iPOT) method was developed by Fang et al.[199] to identify the functional selectivity of a library of opioid ligands for the MOR and determine dynamic mass redistribution (DMR) from the activation of the MOR in living cells. Label-free resonant waveguide grating was used for DMR assays to study HEK-MOR cells with and without preconditioning with probe molecules. Modification of the activity of downstream MOR signaling proteins was accomplished with the assistance of these probe molecules. For the transformation of DMR signals into high-resolution heat maps, a similarity analysis based on a numerical matrix of DMR parameters was used. Data reveals that the iPOT method can characterize the functional selectivity of different MOR signaling pathways among various opioid ligands.[199]

An electrode fabricated by a NiO/CNTs carbon paste and a hydrophilic ionic liquid, 1-methyl-3-butylimidazolium chloride [MBIDZ]Cl has been also used for morphine detection.[200] The maximum irreversible oxidation of morphine was obtained with a cyclic voltammogram at 0.61 V (vs $Ag/AgCl_{sat}$). In comparison with the mere carbon paste electrode, the electrochemical response for morphine was significantly enhanced and oxidation peaks of morphine and diclofenac were displaced by the SWV method. The detection limit for morphine was 0.01×10^{-6} μ in human urine and pharmaceutical samples. Talemi and Mashhadizadeh[201] used the intercalative and electrostatic interaction of morphine with ds-DNA, immobilized on a mercapto-benzaldehyde-improved Au electrode. DPV, under optimal conditions, gave a linear range of 0.05×10^{-6}–500×10^{-6} M and detection limit of 0.01×10^{-6} M for morphine in urine and blood plasma samples.

SPR is another effective technique for the detection of small molecules such as morphine.[202] As an example, Au nanoparticles supported on graphene is one substrate that has been used to incorporate bovine serum albumin-coupled with morphine (BSA-MOR) and antimorphine monoclonal antibody to detect heroin.[203]

In conclusion, amperometric methods and voltammetry techniques are promising for the development of optimal and marketable morphine sensors as they show distinguished detection limits and linear range.

4. Concluding Remarks

The fast, cheap, precise, simple, and portable detection of abused drugs such as cocaine, heroin, and morphine will help to mitigate the adverse impacts of addiction on personal health and society. Given the cost, time, and complexity of classical methods, e.g., chromatography and mass spectrometry, as well as the volume of analyses required for monitoring abused drugs, an alternative approach is needed. Biosensors are a group of emerging analytical tools that offer potential platforms for the detection and quantification of various chemical compounds of interest, including narcotics. Biosensors are promising due to their simplicity, price competitiveness, sensitivity, and portability that enable their potential application as POC devices for drug detection as well as the development and design of sophisticated molecular recognition systems. Although this technology is still in its infancy, several biosensors have been developed and even commercialized for the detection of target analytes, e.g., blood glucose. Among biosensors, aptasensors that utilize optimally engineered aptamers as specific and selective receptors for detecting target molecules can potentially provide the high sensitivity and selectivity required for precise and rapid recognition of abused drugs in medical and forensic applications. Electrochemical biosensors are also very promising for the highly sensitive detection of abused drugs. Such biosensors have been widely studied to detect various drugs especially cocaine. In addition, the synthesis and fabrication of specific materials such as nanoparticles, carbon nanomaterials, screen printed and 3D printed electrodes, as well as electrochemically and fluorimetrically

active tags and agents have facilitated remarkable progress in narcotic biosensing.

Despite intensive ongoing research on biosensors for the detection of narcotic drugs, more research is needed to develop marketable biosensing tools with a competitive price and desirable analytical parameters. Functional nanomaterials such as gold nanoparticles, provide a versatile platform for bioreceptors, especially when functionalized with aptamers, enzymes, and antibodies. The application of next-generation nanoarchitectonics in the development of abuse drug detections may enable a major improvement in selectivity, high sensitivity, ultrafast, and minimalized device fabrication. While aptamers offer affinity binding to specific targets, the reproducibility of biosensors needs to be improved, especially when analyzing complex sample mediums. Sample interference could be eliminated by sample preparation, however, for on-site or POC rapid analysis of samples for monitoring abused drugs, sample pretreatment is not desirable. Electrochemical biosensors have been miniaturized successfully and pave the way for POC devices if existing drawbacks like selectivity and reproducibility can be overcome to improve their analytical performance. With modern advances in the field, we can expect the appearance of biosensors for personal and on-site abused drug monitoring in the coming decade.

Acknowledgements

This work was partially performed at the JST-ERATO Yamauchi Materials Space-Tectonics Project (Grant Number: JPMJER2003) and at the Queensland node of the Australian National Fabrication Facility, a company established under the National Collaborative Research Infrastructure Strategy to provide nano and microfabrication facilities for Australia's researchers. S.V.R. acknowledges the funding from NSF CHE-2032582 and NSF DMR-2011839. E.D. also acknowledges the Japan Society for the Promotion of Science (JSPS) for providing the JSPS standard postdoctoral fellowship. C.H.L also would like to thank the funding support from Ministry of Science and Technology, Taiwan (MOST 110-2222-E-038-002).

Conflict of Interest

The authors declare no conflict of interest.

Keywords

abused drug detection, aptamers, biosensors, nanoarchitectonics, nanoarchitecture

Received: August 12, 2021
Revised: October 14, 2021
Published online:

[1] R. A. Rudd, N. Aleshire, J. E. Zibbell, R. M. Gladden, *Morb. Mortal. Wkly. Rep.* **2016**, *64*, 1378.
[2] C. M. Jones, L. J. Paulozzi, K. A. Mack, *JAMA Intern. Med.* **2014**, *174*, 802.
[3] N. D. Volkow, T. R. Frieden, P. S. Hyde, S. S. Cha, *N. Engl. J. Med.* **2014**, *370*, 2063.
[4] C. M. Jones, J. Logan, R. M. Gladden, M. K. Bohm, *Morb. Mortal. Wkly. Rep.* **2015**, *64*, 719.
[5] S. Y. Hosseini, M. R. Safarinejad, E. Amini, H. Hooshyar, *Eur. Urol. Oncol.* **2010**, *28*, 610.
[6] M. R. Masjedi, P. A. Naghan, S. Taslimi, M. Yousefifard, S. M. Ebrahimi, A. Khosravi, S. Karimi, M. Hosseini, E. Mortaz, *Respiration* **2013**, *85*, 112.
[7] R. Shakeri, R. Malekzadeh, A. Etemadi, D. Nasrollahzadeh, K. Aghcheli, M. Sotoudeh, F. Islami, A. Pourshams, M. Pawlita, P. Boffetta, S. M. Dawsey, C. C. Abnet, F. Kamangar, *Int. J. Cancer* **2013**, *133*, 455.
[8] D. J. Nutt, L. A. King, L. D. Phillips, *Lancet* **2010**, *376*, 1558.
[9] M. Tremlett, B. J. Anderson, A. Wolf, *Paediatr. Anaesth.* **2010**, *20*, 183.
[10] G. M. Robinson, S. Robinson, P. McCarthy, C. Cameron, *N. Z. Med. J.* **2010**, *123*, 59.
[11] M. Van Hout, M. Bergin, M. Foley, E. Rich, A. I. Rapca, R. Harris, I. Norman, presented at *Final Report CODEMISUSED Project European Commission 7th Framework Programme*, Brussels, January **2014**.
[12] T. J. Wiegand, K. M. Babu, *J. Med. Toxicol.* **2016**, *12*, 48.
[13] L. Harper, J. Powell, E. M. Pijl, *Harm Reduct. J.* **2017**, *14*, 52.
[14] S. C. Moldoveanu, *J. Chromatogr. Sci.* **2004**, *42*, 1.
[15] P. Campíns-Falcó, A. Sevillano-Cabeza, R. Herráez-Hernández, C. Molins-Legua, Y. Moliner-Martínez, J. Verdú-Andrés, *Encyclopedia of Analytical Chemistry*, John Wiley & Sons, New York.
[16] A. C. Carpenter, I. T. Paulsen, T. C. Williams, *Genes* **2018**, *9*, 375.
[17] L. Huang, X. Yang, C. Qi, X. Niu, C. Zhao, X. Zhao, D. Shangguan, Y. Yang, *Anal. Chim. Acta* **2013**, *787*, 203.
[18] E. Aydindogan, S. Balaban, S. Evran, H. Coskunol, S. Timur, *Biosensors* **2019**, *9*, 118.
[19] G. G. Guilbault, R. D. Schmid, *Biotechnol. Appl. Biochem.* **1991**, *14*, 133.
[20] S. R. Ahmed, R. Chand, S. Kumar, N. Mittal, S. Srinivasan, A. R. Rajabzadeh, *TrAC, Trends Anal. Chem.* **2020**, *131*, 116006.
[21] R. L. Bunde, E. J. Jarvi, J. J. Rosentreter, *Talanta* **1998**, *46*, 1223.
[22] P. Mehrotra, *J. Oral Biol. Craniofacial Res.* **2016**, *6*, 153.
[23] S. K. Metkar, K. Girigoswami, *Biocatal. Agric. Biotechnol.* **2019**, *17*, 271.
[24] F. Ghorbani, H. Abbaszadeh, J. E. N. Dolatabadi, L. Aghebati-Maleki, M. Yousefi, *Biosens. Bioelectron.* **2019**, *142*, 111484.
[25] P. P. Dillon, S. J. Daly, B. M. Manning, R. O'Kennedy, *Biosens. Bioelectron.* **2003**, *18*, 217.
[26] K. Tappura, I. Vikholm-Lundin, W. M. Albers, *Biosens. Bioelectron.* **2007**, *22*, 912.
[27] K. Besteman, J. -O. Lee, F. G. M. Wiertz, H. A. Heering, C. Dekker, *Nano Lett.* **2003**, *3*, 727.
[28] E. Asadian, M. Ghalkhani, S. Shahrokhian, *Sens. Actuators, B* **2019**, *293*, 183.
[29] M. A. Cooper, *Nat. Rev. Drug Discovery* **2002**, *1*, 515.
[30] A. Antonacci, V. Scognamiglio, V. Mazzaracchio, V. Caratelli, L. Fiore, D. Moscone, F. Arduini, *Front. Bioeng. Biotechnol.* **2020**, *8*, 339.
[31] J. A. Jackman, N. -J. Cho, M. Nishikawa, G. Yoshikawa, T. Mori, L. K. Shrestha, K. Ariga, *Chem. Asian J.* **2018**, *13*, 3366.
[32] R. Tarrahi, Z. Fathi, M. Ö. Seydibeyoğlu, E. Doustkhah, A. Khataee, *Int. J. Biol. Macromol.* **2020**, *146*, 596.
[33] E. Doustkhah, R. Hassandoost, A. Khataee, R. Luque, M. H. N. Assadi, *Chem. Soc. Rev.* **2021**, *50*, 2927.
[34] M. Aono, K. Ariga, *Adv. Mater.* **2016**, *28*, 989.
[35] K. Ariga, M. Aono, *Jpn. J. Appl. Phys.* **2016**, *55*, 1102A1106.
[36] M. Schneiderbauer, M. Emmrich, A. J. Weymouth, F. J. Giessibl, *Phys. Rev. Lett.* **2014**, *112*, 166102.
[37] G. Rapenne, C. Joachim, *Nat. Rev. Mater.* **2017**, *2*, 17040.
[38] K. Ariga, Y. Yamauchi, *Chem. Asian J.* **2020**, *15*, 718.
[39] S. Chenaghlou, A. Khataee, R. Jalili, M. -R. Rashidi, B. Khalilzadeh, S. W. Joo, *Bioelectrochemistry* **2021**, *137*, 107633.
[40] M. Kobya, R. D. C. Soltani, P. I. Omwene, A. Khataee, *Environ. Technol. Innovation* **2020**, *17*, 100519.
[41] M. H. Irani-nezhad, A. Khataee, J. Hassanzadeh, Y. Orooji, *Molecules* **2019**, *24*, 689.

[42] A. Şenocak, A. Khataee, E. Demirbas, E. Doustkhah, *Sens. Actuators, B* **2020**, *312*, 127939.
[43] O. Yağmuroğlu, S. E. Diltemiz, *Anal. Biochem.* **2020**, *591*, 113572.
[44] M. A. P. Mahmud, F. Ejeian, S. Azadi, M. Myers, B. Pejcic, R. Abbassi, A. Razmjou, M. Asadnia, *Chemosphere* **2020**, *259*, 127492.
[45] R. M. Mohamed, F. A. Harraz, *Mater. Res. Bull.* **2020**, *131*, 110965.
[46] L. Fu, Y. Zheng, P. Zhang, H. Zhang, Y. Xu, J. Zhou, H. Zhang, H. Karimi-Maleh, G. Lai, S. Zhao, W. Su, J. Yu, C.-T. Lin, *Biosens. Bioelectron.* **2020**, *159*, 112212.
[47] J. Mohanraj, D. Durgalakshmi, R. A. Rakkesh, S. Balakumar, S. Rajendran, H. Karimi-Maleh, *J. Colloid Interface Sci.* **2020**, *566*, 463.
[48] H. Karimi-Maleh, F. Tahernejad-Javazmi, A. A. Ensafi, R. Moradi, S. Mallakpour, H. Beitollahi, *Biosens. Bioelectron.* **2014**, *60*, 1.
[49] R. Goldoni, M. Farronato, S. T. Connelly, G. M. Tartaglia, W. -H. Yeo, *Biosens. Bioelectron.* **2021**, *171*, 112723.
[50] J. Peterson, G. Vurek, *Science* **1984**, *224*, 123.
[51] M. K. Masud, J. Na, M. Younus, M. S. A. Hossain, Y. Bando, M. J. A. Shiddiky, Y. Yamauchi, *Chem. Soc. Rev.* **2019**, *48*, 5717.
[52] S. Campuzano, J. Wang, *Electroanalysis* **2011**, *23*, 1289.
[53] M. Asif, A. Aziz, M. Azeem, Z. Wang, G. Ashraf, F. Xiao, X. Chen, H. Liu, *Adv. Colloid Interface Sci.* **2018**, *262*, 21.
[54] G. S. Wilson, R. Gifford, *Biosens. Bioelectron.* **2005**, *20*, 2388.
[55] G. S. Wilson, Y. Hu, *Chem. Rev.* **2000**, *100*, 2693.
[56] N. Bhalla, P. Jolly, N. Formisano, P. Estrela, *Essays Biochem.* **2016**, *60*, 1.
[57] G. Das, N. Patra, A. Gopalakrishnan, R. P. Zaccaria, A. Toma, S. Thorat, E. Di Fabrizio, A. Diaspro, M. Salerno, *Analyst* **2012**, *137*, 1785.
[58] H. Qi, M. Li, M. Dong, S. Ruan, Q. Gao, C. Zhang, *Anal. Chem.* **2014**, *86*, 1372.
[59] J. W. Severinghaus, P. B. Astrup, *J. Clin. Monit. Comput.* **1986**, *2*, 125.
[60] L. C. Clark Jr., C. Lyons, *Ann. N. Y. Acad. Sci.* **1962**, *102*, 29.
[61] G. G. Guilbault, J. G. Montalvo, *J. Am. Chem. Soc.* **1969**, *91*, 2164.
[62] S. J. Updike, G. P. Hicks, *Nature* **1967**, *214*, 986.
[63] R. A. Llenado, G. A. Rechnitz, *Anal. Chem.* **1971**, *43*, 1457.
[64] O. Ambartsumyan, D. Gribanyov, V. Kukushkin, A. Kopylov, E. Zavyalova, *Int. J. Mol. Sci.* **2020**, *21*, 3373.
[65] M. Sharifi, S. H. Hosseinali, R. Hossein Alizadeh, A. Hasan, F. Attar, A. Salihi, M. S. Shekha, K. M. Amen, F. M. Aziz, A. A. Saboury, K. Akhtari, A. Taghizadeh, N. Hooshmand, M. A. El-Sayed, M. Falahati, *Talanta* **2020**, *212*, 120782.
[66] R. Bavandpour, M. Rajabi, H. Karimi-Maleh, *New J. Chem.* **2020**, *44*, 11125.
[67] S. Sanli, H. Moulahoum, O. Ugurlu, F. Ghorbanizamani, Z. P. Gumus, S. Evran, H. Coskunol, S. Timur, *Talanta* **2020**, *217*, 121111.
[68] R. Oueslati, C. Cheng, J. Wu, J. Chen, *Biosens. Bioelectron.* **2018**, *108*, 103.
[69] S. Balaban, C. Durmus, E. Aydindogan, Z. P. Gumus, S. Timur, *Electroanalysis* **2020**, *32*, 128.
[70] G. Bozokalfa, H. Akbulut, B. Demir, E. Guler, Z. P. Gumus, D. Odaci Demirkol, E. Aldemir, S. Yamada, T. Endo, H. Coskunol, *Anal. Chem.* **2016**, *88*, 4161.
[71] Y. Fang, X. Huang, Q. Zeng, L. Wang, *Biosens. Bioelectron.* **2015**, *73*, 71.
[72] R. Kawano, T. Osaki, H. Sasaki, M. Takinoue, S. Yoshizawa, S. Takeuchi, *J. Am. Chem. Soc.* **2011**, *133*, 8474.
[73] Q. Sheng, R. Liu, S. Zhang, J. Zheng, *Biosens. Bioelectron.* **2014**, *51*, 191.
[74] Y. Wen, H. Pei, Y. Wan, Y. Su, Q. Huang, S. Song, C. Fan, *Anal. Chem.* **2011**, *83*, 7418.
[75] D. -W. Zhang, C. -J. Sun, F. -T. Zhang, L. Xu, Y. -L. Zhou, X. -X. Zhang, *Biosens. Bioelectron.* **2012**, 31, 363.
[76] C. -Y. Zhang, L. W. Johnson, *Anal.Chem.* **2009**, *81*, 3051.
[77] B. Jiang, M. Wang, Y. Chen, J. Xie, Y. Xiang, *Biosens. Bioelectron.* **2012**, *32*, 305.
[78] M. Hua, P. Li, L. Li, L. Huang, X. Zhao, Y. Feng, Y. Yang, *J. Electroanal. Chem.* **2011**, *662*, 306.
[79] M. Hua, M. Tao, P. Wang, Y. Zhang, Z. Wu, Y. Chang, Y. Yang, *Anal. Sci.* **2010**, *26*, 1265.
[80] F. Li, J. Zhang, X. Cao, L. Wang, D. Li, S. Song, B. Ye, C. Fan, *Analyst* **2009**, *134*, 1355.
[81] J. -L. He, Y.-F. Yang, G.-L. Shen, R.-Q. Yu, *Biosens. Bioelectron.* **2011**, *26*, 4222.
[82] X. Li, H. Qi, L. Shen, Q. Gao, C. Zhang, *Electroanalysis* **2008**, *20*, 1475.
[83] J. Chen, J. Jiang, X. Gao, G. Liu, G. Shen, R. Yu, *Chem. - Eur. J.* **2008**, *14*, 8374.
[84] N. Tavakkoli, N. Soltani, F. Mohammadi, *RSC Adv.* **2019**, *9*, 14296.
[85] J. S. Swensen, Y. Xiao, B. S. Ferguson, A. A. Lubin, R. Y. Lai, A. J. Heeger, K. W. Plaxco, H. T. Soh, *J. Am. Chem. Soc.* **2009**, *131*, 4262.
[86] C. Feng, S. Dai, L. Wang, *Biosens. Bioelectron.* **2014**, *59*, 64.
[87] A. A. Jamali, M. Pourhassan-Moghaddam, J. E. N. Dolatabadi, Y. Omidi, *TrAC, Trends Anal. Chem.* **2014**, *55*, 24.
[88] G. Wang, Y. Wang, L. Chen, J. Choo, *Biosens. Bioelectron.* **2010**, *25*, 1859.
[89] R. Zou, X. Lou, H. Ou, Y. Zhang, W. Wang, M. Yuan, M. Guan, Z. Luo, Y. Liu, *RSC Adv.* **2012**, *2*, 4636.
[90] P. Damborský, J. Švitel, J. Katrlík, *Essays Biochem.* **2016**, *60*, 91.
[91] D. Dey, T. Goswami, *J. Biomed. Biotechnol.* **2011**, 2011, 348218.
[92] R. Eivazzadeh-Keihan, P. Pashazadeh-Panahi, B. Baradaran, M. de la Guardia, M. Hejazi, H. Sohrabi, A. Mokhtarzadeh, A. Maleki, *TrAC, Trends Anal. Chem.* **2018**, *103*, 184.
[93] I. Biran, D. M. Rissin, E. Z. Ron, D. R. Walt, *Anal. Biochem.* **2003**, *315*, 106.
[94] T. Suo, M. Sohail, Y. Ma, B. Li, Y. Chen, X. Zhang, X. Zhou, *Sens. Actuators, B* **2020**, *324*, 128586.
[95] Z. Wu, H. Zhou, Q. Han, X. Lin, D. Han, X. Li, *Analyst* **2020**, *145*, 4664.
[96] M. N. Stojanovic, P. de Prada, D. W. Landry, *J. Am. Chem. Soc.* **2001**, *123*, 4928.
[97] J. Zhou, A. V. Ellis, H. Kobus, N. H. Voelcker, *Anal. Chim. Acta* **2012**, *719*, 76.
[98] Y. Shi, H. Dai, Y. Sun, J. Hu, P. Ni, Z. Li, *Analyst* **2013**, *138*, 7152.
[99] B. Shlyahovsky, D. Li, Y. Weizmann, R. Nowarski, M. Kotler, I. Willner, *J. Am. Chem. Soc.* **2007**, *129*, 3814.
[100] F. Wang, L. Freage, R. Orbach, I. Willner, *Anal. Chem.* **2013**, *85*, 8196.
[101] J. Ge, Z. Liu, X. S. Zhao, *Chin. J. Anal. Chem.* **2012**, *30*, 2023.
[102] Z. Zhou, Y. Du, S. Dong, *Biosens. Bioelectron.* **2011**, *28*, 33.
[103] J. Huang, Y. Chen, L. Yang, Z. Zhu, G. Zhu, X. Yang, K. Wang, W. Tan, *Biosens. Bioelectron.* **2011**, *28*, 450.
[104] S. Niu, X. Lou, Y. Jiang, J. Lin, *Anal. Lett.* **2012**, *45*, 1919.
[105] L. Qiu, H. Zhou, W. Zhu, L. Qiu, J. Jiang, G. Shen, R. Yu, *N. J. Chem.* **2013**, *37*, 3998.
[106] C. Ma, W. Wang, Q. Yang, C. Shi, L. Cao, *Biosens. Bioelectron.* **2011**, *26*, 3309.
[107] C. Wu, L. Yan, C. Wang, H. Lin, C. Wang, X. Chen, C. J. Yang, *Biosens. Bioelectron.* **2010**, *25*, 2232.
[108] J. -L. He, Z. -S. Wu, H. Zhou, H. -Q. Wang, J. -H. Jiang, G. -L. Shen, R. -Q. Yu, *Anal. Chem.* **2010**, *82*, 1358.
[109] A. S. Emrani, N. M. Danesh, M. Ramezani, S. M. Taghdisi, K. Abnous, *Biosens. Bioelectron.* **2016**, *79*, 288.
[110] D. Roncancio, H. Yu, X. Xu, S. Wu, R. Liu, J. Debord, X. Lou, Y. Xiao, *Anal. Chem.* **2014**, *86*, 11100.
[111] L. Gao, W. Xiang, Z. Deng, K. Shi, H. Wang, H. Shi, *Nanomedicine* **2020**, *15*, 325.
[112] F. Yan, Z. Bai, F. Zu, Y. Zhang, X. Sun, T. Ma, L. Chen, *Microchim. Acta* **2019**, *186*, 113.

[113] T. H. Nguyen, S. A. Hardwick, T. Sun, K. T. V. Grattan, *IEEE Sens. J.* **2012**, *12*, 255.
[114] S. P. Wren, T. H. Nguyen, P. Gascoine, R. Lacey, T. Sun, K. T. V. Grattan, *Sens. Actuators, B* **2014**, *193*, 35.
[115] H. Zhang, X. Hu, X. Fu, *Biosens. Bioelectron.* **2014**, *57*, 22.
[116] S. Wang, G. Zhang, Q. Chen, J. Zhou, Z. Wu, *Microchim. Acta* **2019**, *186*, 724.
[117] Q. Cai, L. Chen, F. Luo, B. Qiu, Z. Lin, G. Chen, *Anal. Bioanal. Chem.* **2011**, *400*, 289.
[118] B. Sun, H. Qi, F. Ma, Q. Gao, C. Zhang, W. Miao, *Anal. Chem.* **2010**, *82*, 5046.
[119] Y. Li, X. Ji, B. Liu, *Anal. Bioanal. Chem.* **2011**, *401*, 213.
[120] O. Adegoke, C. McKenzie, N. N. Daeid, *Sens. Actuators, B* **2019**, *287*, 416.
[121] K. Li, W. Qin, F. Li, X. Zhao, B. Jiang, K. Wang, S. Deng, C. Fan, D. Li, *Angew. Chem., Int. Ed.* **2013**, *52*, 11542.
[122] J. Liu, Y. Lu, *Angew. Chem., Int. Ed.* **2006**, *45*, 90.
[123] J. Zhang, L. Wang, D. Pan, S. Song, F. Y. C. Boey, H. Zhang, C. Fan, *Small* **2008**, *4*, 1196.
[124] J. E. Smith, D. K. Griffin, J. K. Leny, J. A. Hagen, J. L. Chávez, N. Kelley-Loughnane, *Talanta* **2014**, *121*, 247.
[125] G. Klenkar, B. Liedberg, *Anal. Bioanal. Chem.* **2008**, *391*, 1679.
[126] F. Luo, L. Zheng, S. Chen, Q. Cai, Z. Lin, B. Qiu, G. Chen, *Chem. Commun.* **2012**, *48*, 6387.
[127] Q. Yu, J. Zhu, Z. Xu, X. Huang, *Sens. Actuators, B* **2015**, *213*, 27.
[128] M. A. D. Neves, C. Blaszykowski, S. Bokhari, M. Thompson, *Biosens. Bioelectron.* **2015**, *72*, 383.
[129] B. R. Srijanto, C. P. Cheney, D. L. Hedden, A. C. Gehl, P. B. Crilly, M. A. Huestis, T. L. Ferrell, *Sens. Lett.* **2012**, *10*, 850.
[130] K. Kang, A. Sachan, M. Nilsen-Hamilton, P. Shrotriya, *Langmuir* **2011**, *27*, 14696.
[131] J. Halámek, A. Makower, K. Knösche, P. Skládal, F. W. Scheller, *Talanta* **2005**, *65*, 337.
[132] J. Ngeh-Ngwainbi, A. A. Suleiman, G. G. Guilbault, *Biosens. Bioelectron.* **1990**, *5*, 13.
[133] K. -K. Liu, R. -G. Wu, Y. -J. Chuang, H. S. Khoo, S. -H. Huang, F.-G. Tseng, *Sensors* **2010**, *10*, 6623.
[134] G. Luka, A. Ahmadi, H. Najjaran, E. Alocilja, M. DeRosa, K. Wolthers, A. Malki, H. Aziz, A. Althani, M. Hoorfar, *Sensors* **2015**, *15*, 30011.
[135] M. Calleja, M. Nordström, M. Álvarez, J. Tamayo, L. M. Lechuga, A. Boisen, *Ultramicroscopy* **2005**, *105*, 215.
[136] N. V. Lavrik, M. J. Sepaniak, P. G. Datskos, *Rev. Sci. Instrum.* **2004**, *75*, 2229.
[137] L. A. Pinnaduwage, T. Thundat, A. Gehl, S. D. Wilson, D. L. Hedden, R. T. Lareau, *Ultramicroscopy* **2004**, *100*, 211.
[138] T. Frisk, D. Rönnholm, W. van der Wijngaart, G. Stemme, *Lab Chip* **2006**, *6*, 1504.
[139] O. Havakuk, S. H. Rezkalla, R. A. Kloner, *Circulation* **2017**, *70*, 101.
[140] J. Akwe, *J. Lung Pulm. Respir. Res.* **2017**, *4*, 00121.
[141] J. A. Madden, R. H. Powers, *Life Sci.* **1990**, *47*, 1109.
[142] J. R. Woods, M. A. Plessinger, K. E. Clark, *J. Am. Med. Assoc.* **1987**, *257*, 957.
[143] J. Vicente, L. Wiessing, *Eurosurveillance* **2007**, *12*, 3317.
[144] S. B. Zhang, P. Z. Han, P. Lu, X. Hu, L. Y. Zheng, X. W. Liu, G. Y. Shen, J. L. Lu, L. P. Qiu, S. B. Zhou, *Adv. Mater. Res.* **2013**, *791–793*, 988.
[145] Y. Zhao, X. -W. He, X. -B. Yin, *Chem. Commun.* **2011**, *47*, 6419.
[146] M. N. Stojanovic, D. W. Landry, *J. Am. Chem. Soc.* **2002**, *124*, 9678.
[147] R. Freeman, Y. Li, R. Tel-Vered, E. Sharon, J. Elbaz, I. Willner, *Analyst* **2009**, *134*, 653.
[148] M. N. Stojanovic, P. de Prada, D. W. Landry, *J. Am. Chem. Soc.* **2000**, *122*, 11547.
[149] R. J. White, N. Phares, A. A. Lubin, Y. Xiao, K. W. Plaxco, *Langmuir* **2008**, *24*, 10513.
[150] B. R. Baker, R. Y. Lai, M. S. Wood, E. H. Doctor, A. J. Heeger, K. W. Plaxco, *J. Am. Chem. Soc.* **2006**, *128*, 3138.
[151] D. Li, S. Song, C. Fan, *Acc. Chem. Res.* **2010**, *43*, 631.
[152] H. Li, P. Dauphin-Ducharme, G. Ortega, K. W. Plaxco, *J. Am. Chem. Soc.* **2017**, *139*, 11207.
[153] S. M. Taghdisi, N. M. Danesh, A. S. Emrani, M. Ramezani, K. Abnous, *Biosens. Bioelectron.* **2015**, *73*, 245.
[154] F. Xia, X. Zuo, R. Yang, R. J. White, Y. Xiao, D. Kang, X. Gong, A. A. Lubin, A. Vallée-Bélisle, J. D. Yuen, *J. Am. Chem. Soc.* **2010**, *132*, 8557.
[155] K. Yang, C. -Y. Zhang, *Anal. Chem.* **2010**, *82*, 9500.
[156] Y. Li, H. Qi, Y. Peng, J. Yang, C. Zhang, *Electrochem. Commun.* **2007**, *9*, 2571.
[157] T. Man, W. Lai, M. Xiao, X. Wang, A. R. Chandrasekaran, H. Pei, L. Li, *Biosens. Bioelectron.* **2020**, *147*, 111742.
[158] Y. Tang, F. Long, C. Gu, C. Wang, S. Han, M. He, *Anal. Chim. Acta* **2016**, *933*, 182.
[159] A. R. Toppozada, J. Wright, A. T. Eldefrawi, M. E. Eldefrawi, E. L. Johnson, S. D. Emche, C. S. Helling, *Biosens. Bioelectron.* **1997**, *12*, 113.
[160] B. Wenger, K. Kugelbrey, H. Gao, H. Sigrist, G. Voirin, *Biosens. Bioelectron.* **2012**, *34*, 94.
[161] F. Xia, X. Zuo, R. Yang, Y. Xiao, D. Kang, A. Vallée-Bélisle, X. Gong, J. D. Yuen, B. B. Hsu, A. J. Heeger, *Proc. Natl. Acad. Sci. USA* **2010**, *107*, 10837.
[162] D. Zheng, R. Zou, X. Lou, *Anal. Chem.* **2012**, *84*, 3554.
[163] C. Teller, J. Halámek, J. Žeravík, W. F. Stöcklein, F. W. Scheller, *Biosens. Bioelectron.* **2008**, *24*, 111.
[164] P. L. Voyvodic, A. Pandi, M. Koch, I. Conejero, E. Valjent, P. Courtet, E. Renard, J. -L. Faulon, J. Bonnet, *Nat. Commun.* **2019**, *10*, 1.
[165] J. Wang, J. Hou, H. Zhang, Y. Tian, L. Jiang, *ACS Appl. Mater. Interfaces* **2018**, *10*, 2033.
[166] L. Asturias-Arribas, M. A. Alonso-Lomillo, O. M. J. Domínguez-Renedo, *Talanta* **2013**, *111*, 8.
[167] L. Asturias-Arribas, M. A. Alonso-Lomillo, O. M. J. Domínguez-Renedo, *Talanta* **2014**, *129*, 315.
[168] W. C. DeLoache, Z. N. Russ, L. Narcross, A. M. Gonzales, V. J. J. Martin, J. E. Dueber, *Nat. Chem. Biol.* **2015**, *11*, 465.
[169] A. A. Ensafi, E. Heydari-Bafrooei, B. Rezaei, *Biosens. Bioelectron.* **2013**, *41*, 627.
[170] P. J. Holt, L. D. G. Stephens, N. C. Bruce, C. R. Lowe, *Biosens. Bioelectron.* **1995**, *10*, 517.
[171] J. P. Hart, A. Crew, E. Crouch, K. C. Honeychurch, R. M. Pemberton, *Anal. Lett.* **2004**, *37*, 789.
[172] X. Niu, L. Huang, J. Zhao, M. Yin, D. Luo, Y. Yang, *Anal. Methods* **2016**, *8*, 1091.
[173] M. Saberian, D. Asgari, Y. Omidi, J. Barar, H. Hamzeiy, *Turk. J. Chem.* **2013**, *37*, 366.
[174] T. Zhou, H. Yu, Q. Hu, Y. Fang, *J. Pharm. Biomed. Anal.* **2002**, *30*, 13.
[175] S. S. Martins, A. Sarvet, J. Santaella-Tenorio, T. Saha, B. F. Grant, D. S. Hasin, *JAMA Psychiatry* **2017**, *74*, 445.
[176] B. K. Madras, *JAMA Psychiatry* **2017**, *74*, 441.
[177] L. Scholl, P. Seth, M. Kariisa, N. Wilson, G. Baldwin, *Morb. Mortal. Wkly. Rep.* **2019**, *67*, 1419.
[178] R. M. Gladden, P. Martinez, P. Seth, *Morb. Mortal. Wkly. Rep.* **2016**, *65*, 837.
[179] P. -J. Holt, N. C. Bruce, C. R. Lowe, *Anal. Chem.* **1996**, *68*, 1877.
[180] D. A. Rathbone, P. J. HOLT, N. C. Bruce, C. R. Lowe, *Ann. N. Y. Acad. Sci.* **1996**, *782*, 534.
[181] A. Navaee, A. Salimi, H. Teymourian, *Biosens. Bioelectron.* **2012**, *31*, 205.
[182] Z. -Y. Shang, H. Chao-Feng, S. Qi-Jun, *Chin. J. Anal. Chem.* **2014**, *42*, 904.
[183] J. Tey, S. Gandhi, I. Wijaya, A. Palaniappan, J. Wei, I. Rodriguez, C. Suri, S. Mhaisalkar, *Small* **2010**, *6*, 993.
[184] F. Wang, J. Meng, L. Zhang, T. Johnson, C. Chen, S. Roy, *Sci. Rep.* **2018**, *8*, 3596.

[185] J. Tey, I. Wijaya, S. Gandhi, J. Wei, I. Rodriguez, C. Suri, S. Mhaisalkar, *TechConnect Briefs* **2010**, *1*, 187190.
[186] E. Doustkhah, M. Farajzadeh, H. Mohtasham, J. Habeeb, S. Rostamnia, Handbook of Graphene, (Eds: E. Celasco, A. N. Chaika, T. Stauber, M. Zhang, C. Ozkan, C. Ozkan, U. Ozkan, B. Palys, S. W. Harun), Wiley-VCH, Weinheim, Germany **2019**, pp. 529–558.
[187] S. Rostamnia, B. Zeynizadeh, E. Doustkhah, H. G. Hosseini, *J. Colloid Interface Sci.* **2015**, *451*, 46.
[188] S. Rostamnia, E. Doustkhah, Z. Karimi, S. Amini, R. Luque, *ChemCatChem* **2015**, *7*, 1678.
[189] E. Doustkhah, Y. Ide, *ACS Appl. Nano Mater.* **2019**, *2*, 7513.
[190] G. Maccaferri, F. Terzi, Z. Xia, F. Vulcano, A. Liscio, V. Palermo, C. Zanardi, *Sens. Actuators, B* **2019**, *281*, 739.
[191] R. Abe, H. Ohashi, I. Iijima, M. Ihara, H. Takagi, T. Hohsaka, H. Ueda, *J. Am. Chem. Soc.* **2011**, *133*, 17386.
[192] H. Ahmar, H. Tabani, M. H. Koruni, S. S. H. Davarani, A. R. Fakhari, *Biosens. Bioelectron.* **2014**, *54*, 189.
[193] M. Matsukizono, M. Kamegawa, K. Tanaka, S. Kohra, K. Arizono, Y. Hamazoe, K. Sugimura, *Antibodies* **2013**, *2*, 93.
[194] P. P. Dillon, B. M. Manning, S. J. Daly, A. J. Killard, R. O'Kennedy, *J. Immunol. Methods* **2003**, *276*, 151.
[195] P. P. Dillon, A. J. Killard, S. J. Daly, P. Leonard, R. O'Kennedy, *J. Immunol. Methods* **2005**, *296*, 77.
[196] A. A. Ensafi, M. Izadi, B. Rezaei, H. Karimi-Maleh, *J. Mol. Liq.* **2012**, *174*, 42.
[197] P. Jinyin, Y. Ya, T. Yifeng, *J. Electrochem. Soc.* **2015**, *162*, B207.
[198] D. Kriz, K. Mosbach, *Anal. Chim. Acta* **1995**, *300*, 71.
[199] M. Morse, E. Tran, H. Sun, R. Levenson, Y. Fang, *PLoS One* **2011**, *6*, e25643.
[200] A. L. Sanati, H. Karimi-Maleh, A. Badiei, P. Biparva, A. A. Ensafi, *Mater. Sci. Eng. C* **2014**, *35*, 379.
[201] R. P. Talemi, M. H. Mashhadizadeh, *Talanta* **2015**, *131*, 460.
[202] J. Mitchell, *Sensors* **2010**, *10*, 7323.
[203] S. Eissa, M. Zourob, *Microchim. Acta* **2017**, *184*, 2281.

Rasoul Moradi received his Ph.D. degree in chemical engineering-nanotechnology from the University of Tehran in 2016. Currently, he is an associate professor at Khazar University, Azerbaijan. His research group focus around the questions about nanoenabled water and energy systems, fluid flow, and nanobio-coupled systems. He has published more than 100 scientific articles and organized various international conferences in nanotechnology and nonscience.

Esmail Doustkhah received his Ph.D. in 2017. During his Ph.D. studies, he was awarded several prizes, scholarships and internships, including a visiting research position and an internship at the National Institute for Materials Science (NIMS), Japan. In 2018, he was accepted as a postdoctoral researcher at NIMS, working on mesoporous and 2D materials. In late 2019, he was awarded the Japan Society for the Promotion of Science (JSPS) fellowship in Japan. His current research interests are focused on the development of new porous and layered materials and studying their (photo)(bio)catalytic features.

Yusuke Yamauchi received his Ph.D. in 2007 and joined the National Institute of Materials Science (NIMS), Japan. In 2016, he was granted the ARC Future Fellowship and joined the University of Wollongong. Since 2018, he has moved to the University of Queensland as Senior Group Leader. He serves as an ERATO Research Director, a Group Leader at NIMS, a Visiting Professor at the Waseda University, an Advisory Board Member in several journals, and an Associate Editor of the Journal of Materials Chemistry A and Chemical Engineering Journal. He is a Highly-Cited Researcher from 2016-2021 (>50,000 citations, h-index > 120).

Slava V. Rotkin is a Frontier Professor of Engineering Science & Mechanics at Penn State University. He received Ph.D. in Physics & Mathematics from Ioffe Institute. Rotkin served as an ECS Board of Directors member and is the ECS NANO Division Treasurer and Senior Advancement Officer. He is a Fellow of the Electrochemical Society and recipient of several scientific awards, including Hillman Award, Class of '68 Fellowship, Libsch Early Career Research Award, Feigl Junior Faculty Chair, Beckman Fellowship. Rotkin is an editor of three books and author of 170+ papers and proceedings focused on near-field optics, plasmonics, nanobiophysics, and 2D quantum materials.